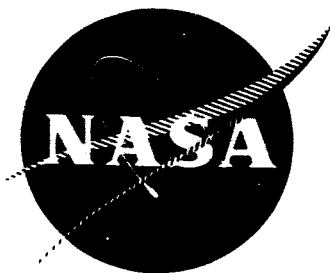


K.

NASA CR-54432



MIXING AND HEAT TRANSFER OF AN ARGON ARCJET
WITH A COAXIAL FLOW OF COLD HELIUM

by

Jerry Grey, Peter M. Williams, and David B. Fradkin

prepared for

NATIONAL AERONAUTICS AND SPACE ADMINISTRATION

CONTRACT NAS 3-3680

FACILITY FORM 802	N66 37643	
	(ACCESSION NUMBER)	(THRU)
	66	1
	(PAGES)	(CODE)
CR-54432	28	
	(NASA CR OR TMX OR AD NUMBER)	(CATEGORY)

PRINCETON UNIVERSITY

Department of
Aerospace and Mechanical Sciences

GPO PRICE	\$	_____
CFSTI PRICE(S)	\$	_____
Hard copy (HC)		\$ 3.00
Microfiche (MF)		.75

NOTICE

This report was prepared as an account of Government sponsored work. Neither the United States, nor the National Aeronautics and Space Administration (NASA), nor any person acting on behalf of NASA:

- A.) Makes any warranty or representation, expressed or implied, with respect to the accuracy, completeness, or usefulness of the information contained in this report, or that the use of any information, apparatus, method, or process disclosed in this report may not infringe privately owned rights; or
- B.) Assumes any liabilities with respect to the use of, or for damages resulting from the use of any information, apparatus, method or process disclosed in this report.

As used above, "person acting on behalf of NASA" includes any employee or contractor of NASA, or employee of such contractor, to the extent that such employee or contractor of NASA, or employee of such contractor prepares, disseminates, or provides access to, any information pursuant to his employment or contract with NASA, or his employment with such contractor.

Requests for copies of this report should be referred to

National Aeronautics and Space Administration
Office of Scientific and Technical Information
Attention: AFSS-A
Washington, D.C. 20546

FINAL REPORT

MIXING AND HEAT TRANSFER OF AN ARGON ARCJET

WITH A COAXIAL FLOW OF COLD HELIUM

by

Jerry Grey, Peter M. Williams, and David B. Fradkin

Aeronautical Engineering Laboratory

prepared for

NATIONAL AERONAUTICS AND SPACE ADMINISTRATION

October 31, 1964

CONTRACT NAS 3-3680

Technical Management

NASA Lewis Research Center

Cleveland, Ohio

Robert G. Ragsdale

Nuclear Reactor Division

Princeton University

Department of Aerospace and Mechanical Sciences

TABLE OF CONTENTS

	<u>PAGE</u>
TITLE PAGE	1
CONTENTS	2
LIST OF ILLUSTRATIONS	3
I. SUMMARY	5
II. INTRODUCTION	6
A. Purpose	6
B. Background	7
III. DESCRIPTION OF TEST PROGRAM	8
A. Apparatus	8
1. Plasma Generator	8
2. Duct and Test Section	10
3. Instrumentation	11
B. Conduct of Tests	14
1. Visual Studies	14
2. Detailed Surveys	16
IV. DISCUSSION OF RESULTS	17
A. Visual Studies	17
B. Detailed Mapping of Flow Field	18
C. Effects of Turbulence	19
D. Variations of Core Jet Mass Flow	24
V. CONCLUSIONS	24
REFERENCES	27

LIST OF ILLUSTRATIONS

	<u>PAGE</u>
1. Diagram of Apparatus	28
2. Thermal Dynamics F-80 Arcjet Torch with Swirl Plate and Cathode	29
3. Nozzle-Anode Used with F-80 Arcjet Torch	30
4. Creare Plasma Generator	31
5. Adaptor and Light-Gas Injection Plate	32
6. Creare Generator Installed in Test Apparatus	33
7. View of Round Vycor Duct Used for Visual Coaxial-Flow Transition Studies	34
8. View of Square Duct Used for Coaxial -Flow Transition Studies by Schlieren Photography	35
9. View of Calorimetric Duct Used for Detailed Coaxial-Flow Mixing and Heat Transfer Experiment	36
10. Traveling Schlieren System	37
11. Diagram of Calorimetric Probe	38
12. Diagram of Instrumentation Used with Tare- Measurement Calorimetric Probe to Measure Enthalpy, Velocity, and Gas Composition	39
13. Schlieren Photographs of a Free Argon Arcjet in Nitrogen	40
14. Schlieren Photographs of Argon Arcjet in Nitrogen in 3-Inch Square Duct	41
15. Visual Length of Laminar Arcjet versus Reynolds Number of Coaxial Gas	42
16. Visual Length of Laminar Arcjet versus Velocity of Coaxial Gas	43
17. Schlieren Photographs Showing Scale of Tur- bulence in Coaxial Helium Flow	44

LIST OF ILLUSTRATIONS

	<u>PAGE</u>
18. Centerline Temperature Versus Axial Position	45
19. Centerline Velocity Versus Axial Position	46
20. Centerline Helium Concentration Versus Axial Position	47
21. Centerline Enthalpy Versus Axial Position	48
22. Temperature, Velocity and Composition Profiles at Nozzle Exit Plane	49
23. Temperature, Velocity and Composition Profiles at 1/2 Inch Downstream from Nozzle Exit Plane	50
24. Temperature, Velocity and Composition Profiles at 1 Inch Downstream from Nozzle Exit Plane	51
25. Temperature, Velocity and Composition Profiles at 2 Inches Downstream from Nozzle Exit Plane	52
26. Temperature, Velocity and Composition Profiles at 3 Inches Downstream from Nozzle Exit Plane	53
27. Temperature, Velocity and Composition Profiles at 5 Inches Downstream from Nozzle Exit Plane	54
28. Temperature Profile at 1 Inch Downstream from Nozzle Exit Plane for Variable Argon Flow Rate	55
29. Velocity Profile at 1 Inch Downstream from Nozzle Exit Plane for Variable Argon Flow Rate	56
30. Composition Profile at 1 Inch Downstream from Nozzle Exit Plane for Variable Argon Flow Rate	57

I. SUMMARY

The mixing of a subsonic, one-centimeter-diameter argon arcjet with a coaxial flow of cold helium in a 3-inch-diameter duct has been studied visually by schlieren photography and quantitatively with a 0.075-inch-diameter calorimetric and sampling probe. Measurements of temperature, velocity and composition of the mixing field were made for an initially laminar argon jet having a mass flow of 0.3 gm/sec, an exit plane peak temperature of 20,000°R, and an exit plane peak velocity of 600 ft/sec. The effects of cold coaxial helium flow velocities of 0, 0.27, and 2.7 ft/sec on jet mixing characteristics were studied, as well as the effect on the flow field of varying the argon jet flow from 0.2 to 1.4 grams per second at a fixed coaxial helium velocity of 0.27 ft/sec.

The data have been correlated with previous experimental and theoretical investigations for a free argon arcjet at similar initial conditions, mixing with stagnant helium at 1 atmosphere. The results are in excellent agreement with this earlier work. The principal effect of the controlled ducted coaxial flow has been to hasten mixing by causing earlier transition of the arcjet to turbulence. The dominant mixing process for both the free and ducted jets was found to be the inflow of helium into the argon jet, the effects of radiation and ionization being negligible. This results from the high specific heat and high diffusion coefficient of helium at arcjet temperatures. In cases where turbulence is present, the dominant mixing process is still the inflow of helium, although the rate of this inflow

is substantially augmented by turbulence.

The experiments with variable argon mass flow showed that at increased argon mass flows the rate of mixing of the jet is retarded, a phenomenon commonly observed in other types of jets.

The results indicate potential feasibility of the coaxial gaseous-core nuclear rocket. The observed mechanism of jet cooling and mixing, which consists principally of an inflow of light helium atoms rather than the dispersion of the heavier argon atoms, is consistent with the requirements for retention of gaseous nuclear fuel in this concept. In the rocket, however, the coaxial light gas velocity is substantially greater than the core velocity, and it is this case which will be investigated in future work with the object of determining whether the light-gas inflow mechanism will continue to be observed under these conditions.

II. INTRODUCTION

A. Purpose

The purpose of this program, as defined in Reference 1, was "to investigate the mixing and heat transfer characteristics of a hot, high-molecular-weight gas jet injected into a bounded annular flow of a surrounding cool, low-molecular-weight gas. Of specific interest are the axial pressure distribution, the effect of outer-stream turbulence on transition of the inner jet, and the effect of heat-release via ion recombination in the inner jet."

In detail, again quoting from Reference 1,

"1. Data from measurements are for use with an analysis made at NASA Lewis. The system is basically a plasma jet injected into an outer, room-temperature gas.

2. The outer gas shall be of low molecular weight (helium) and the plasma of high molecular weight (argon).

3. The light gas shall be contained within a channel whose diameter is approximately five times that of the plasma.

4. The plasma shall be injected into the light gas at velocities down to the same as that of the light gas, as limited by experimentally obtainable conditions.

5. The results shall be presented as measured values of concentration, temperature, and velocity taken at various radial positions. These radial profiles shall be measured at various distances downstream from the point of injection of the inner gas.

6. The above measurements shall be made over a range of gas flow rates such that Reynolds numbers of the inner stream shall be between 100 and 1,000, and the Reynolds numbers of the outer stream shall be between 50 and 10,000, as limited by experimentally obtainable conditions."

B. Background

Knowledge of the nature of the flow processes occurring in the coaxial-geometry gaseous-core nuclear rocket² is required in order to properly evaluate the feasibility of this propulsion concept. Although analytical models and analyses

have been formulated for both laminar³ and turbulent^{4,5} flows, it was necessary to obtain some experimental indication of their validity. The equipment previously developed at Princeton^{6,7} for more generalized studies of high-temperature, partly-ionized gas interactions^{8,9} appeared to be well suited to this purpose, and with comparatively minor additions and modifications, was adaptable to the purposes described above.

III. DESCRIPTION OF TEST PROGRAM

A. Apparatus

The entire experimental apparatus is diagrammed in Figure 1. It consists of a plasma generator mounted so as to eject a partly-ionized gas jet horizontally into a test chamber, the test chamber itself forming part of a 1,000-gallon tank. For the purposes of these tests, a series of ducts could be mounted which permitted the injection of a coaxial flow of cool gas, concentric with the plasma jet axis. Instrumentation consisted of a schlieren system for visual studies, a calorimetric probe⁶ and drive systems suitable for pressure, composition and enthalpy mapping of the entire duct interior, and miscellaneous instrumentation related to the arc generator and duct. Details of each major component are described in the ensuing paragraphs.

1. Plasma Generator

The initial visual studies, as originally planned, were made with a Plasmaflame Model F-80 Arcjet manufactured by Thermal Dynamics, Inc., (Figure 2). This generator

was available at Princeton, and for the purpose of these tests utilized a 3/8"-diameter straight-bore water-cooled nozzle, whose exterior was tapered so as to provide smooth-entry mixing with the annular light-gas flow (Figure 3).

The torch was powered by a marine diesel generator driving four Westinghouse RA-2 rectifiers, one of which was provided with remote current adjustment, having a total DC capacity (after power factor and lead losses) of approximately 75 kw. A water-cooled, copper-tipped prod was used for torch starting, and operation was controlled from a modified Thermal Dynamics console. The torch, nozzle and leads were cooled with 300 psi water from a Pesco gear pump. Calorimetric measurement of the rate of heat extraction from the torch by the coolant was available.

As described below, it was later found visually that the laminar jet obtained with the Thermal Dynamics torch was too unstable for probe profile measurements. A new plasma generator was procured for use in a complementary Air Force research program. This new generator, (Figure 4) manufactured by Creare, Inc., was adaptable to the existing power supply, ducts, and test chamber. Its principal advantages were (a) micrometer adjustment of radial and axial cathode position; (b) a sectioned straight-line nozzle consisting of a series of thin insulated segments, one of which could be grounded so that the anode arc contact point could be pre-selected and maintained. This generator provided excellent

laminar stability under nearly all operating conditions, and was used to collect the probe test data described later.

An adapter and light-gas injection plate compatible with the duct were designed and installed for this generator (Figure 5). The injection plate, which covered the entire duct inlet, was uniformly drilled with small holes to provide approximately uniform flow of the light gas.

The test gases used were argon for the hot gas and helium for the cool gas. Several test runs were also made using nitrogen for the cool gas for reasons to be discussed later.

✓ 2. Duct and Test Section

The test section consisted of a rectangular parallelepiped 18" square by 3 feet long, opening into a 1,000-gallon commercial gasoline tank internally braced for vacuum operation (see Figure 6). The test section was equipped with quartz windows for viewing either the open plasmajet exhaust or the duct. The plasma generator and duct were mounted on opposite sides of the test section endplate, as shown in Figure 6, with the duct fully contained within the test section. Two conventional mechanical vacuum pumps connected to the tank could provide test section pressures down to about 1^μ Hg absolute. The tank pressure was prevented from exceeding one atmosphere (absolute) by a large flapper. A telescope mounted in the far end of the tank, opposite the duct and arcjet, provided capability for viewing the arc during operation.

Three different ducts were used for this test program. A cylindrical Vycor duct (Figure 7) was first constructed to provide visual indication of the nature of the jet mixing region. Although this was suitable for direct viewing, the curvature of the Vycor precluded the use of schlieren photography. Consequently, a metal duct of square cross-section having approximately the same dimensions (3") and fitted with flat quartz windows (Figure 8) was used for photographic recording of the mixing region, as will be described in Section III-B. Correlation between the two ducts is also described later.

Detailed flow-parameter surveys were made in a brass calorimetric duct (Figure 9) designed to provide two-dimensional coverage of the entire duct interior by the calorimetric probe. This duct was water-cooled, permitting measurement of the overall heat transfer to the duct walls.

3. Instrumentation

The two unique items of instrumentation required for the subject program were the schlieren system and the calorimetric probe. Other more or less standard items, which included those necessary for measurements of arcjet power, gas flow rates, tank pressures, etc., are not described in detail here.

(a) Schlieren System

In order to establish the general nature of the flow within the duct (i.e., length of laminar core, location of transition, structure and stability of the laminar core flow,

etc.), the existing schlieren system of Figure 10 was used, together with the flat-sided duct of Figure 8. The system was of standard design, employing parabolic mirrors instead of lenses in order to gain light-path length, and utilizing a BH-6 microsecond spark source with an open-shutter camera in order to obtain sufficient illumination to provide transparency of the intensely luminous arcjet.

The system was adequate to yield good schlieren photographs when the hot argon jet issued into cold nitrogen. The quality was barely adequate, however, when the jet was cooled by helium, since the density of the hot argon was sufficiently close to that of the coaxial helium so that the density gradients were at the limits of the systems resolution.

(b) Calorimetric Probe

The calorimetric probe is an instrument which measures enthalpy, stagnation pressure, and composition of gases at temperatures up to at least 25,000°F. It has been used for some time in arcjet diagnosis, and since it has been described in detail elsewhere⁶⁻¹⁰, only its general nature is outlined here.

The probe configuration and its associated instrumentation are diagrammed in Figures 11 and 12, respectively. The construction of the probe itself is of copper, with a brass base. Cooling water from a high-pressure source (up to 1,000 psi) enters through the mounting block, passes through the outer

channel to the tip, and leaves via the inner channel. Sheathed, ungrounded thermocouple junctions are located where the probe cooling water flow enters and leaves the sampling tube. A steady flow of sample gas can be drawn by a vacuum pump from the probe tip, through the central tube past a thermocouple junction located in the tube, and then through the support shaft to valving and instrumentation.

The flow of the hot sample gas in the central tube causes the probe cooling water to rise in temperature a greater amount than when the gas sample flow is not permitted to flow through the tube. A flowmeter measures the probe coolant flow and a critical orifice measures the gas flow. These measurements are sufficient to compute the enthalpy of the gas sample at the point where it enters the probe.

The composition of the two-component gas sample is determined by measuring its thermal conductivity in a carefully calibrated commercial cell, and stagnation pressure is measured when the gas sample is not flowing by simply diverting, through appropriate valving, the gas sample line from the vacuum pump to a water manometer. Enthalpy can be converted to temperature, once the gas composition is known, from an equilibrium theory such as the Saha equation. The measured stagnation pressure is converted to velocity using the Bernoulli equation, since the gas Mach number is less than 0.1.

The sensitivity and calibration of the probe under similar experimental conditions have been described elsewhere⁹.

In previous work, energy and mass balances showed that the probe's accuracy (standard deviation from the mean) was about 3 per cent.⁶

B. Conduct of Tests

1. Visual Studies

The visual studies were undertaken with the dual objective of (a) establishing the general character of the jet mixing as a guide to the ensuing probe measurements, and (b) establishing that the jet was sufficiently stable and uniform that worthwhile and reproducible probe data could be obtained. Findings in accordance with this latter objective resulted in postponing the probe measurements until the new Creare plasma generator could be installed, as was described previously. The majority of the visual experiments were made with the Thermal Dynamics torch, and although the flame was not sufficiently steady for detailed probing, it was satisfactory from the standpoint of establishing the general nature of the flow.

The first series of visual studies was made in the round Vycor duct, and data were obtained using both helium and nitrogen as the coaxial gas. The conduct of the experiments was generally the same for both gases. The test chamber and the 1000-gallon exhaust tank were evacuated to about 1/5 atmosphere, since it was found experimentally that longer laminar flames, and thus greater flame length differences, could be obtained at reduced pressure. It was believed that this would not invalidate the visual data, since the purpose

of the visual study was only to establish trends to be later verified by probe measurements at one atmosphere.

Once the proper test chamber pressure was established, the plasma generator was started and adjusted to produce as long a laminar flame as possible. Most of these tests were run with an argon flow of about 100 SCFH at a net plasma generator power of about 19 kw.

With the arcjet thus adjusted, observations were made of the character of the jet for different coaxial gas velocities. The typical observation procedure was to first observe the flame with no coaxial gas flow, and record the full length of the laminar portion of the jet. The coaxial flow was then initiated, and the new length of the laminar portion of the jet was observed, together with the flow rate of the coaxial gas. Observations were continued at increasingly higher coaxial flows until the laminar jet disappeared and turbulence was observed at the nozzle exit plane.

These visual observations were made with the aid of schlieren photography, to define as nearly as possible the exact length of the laminar jet. Figure 13 is a schlieren photograph illustrating a typical laminar arcjet and its transition to turbulence in a free environment. Figure 14 is a schlieren photograph of laminar and turbulent jets taken through the windows of the square three-inch duct. Although the quality of these latter photographs is not as good as for the free jet, the difference between laminar and turbulent flows can be clearly distinguished. Note from

Figure 14 that turbulence can exist right at the nozzle exit plane.

As stated previously, schlieren photographs could not be taken through the round duct. The photographs taken in the square duct were therefore used to confirm the round-duct visual observations. Data were taken with both helium and nitrogen coaxial flows, in both round and square ducts, and also with a free jet in nitrogen.

2. Detailed Surveys

The probe measurements were conducted in the calorimetric duct of Figure 9. Radial profile measurements were taken at the exit plane at quarter-inch intervals to the point at which the jet had become fully turbulent and full mixing of the arcjet with the coaxial gas flow had been completed.

Profile data were taken under the following initial conditions for the argon jet:

Plasma generator power	14 kw
Argon Mass Flow Rate	0.323 gm/sec
Jet Temperature at Nozzle Exit*	20,000°R
Initial Jet Velocity*	600 ft/sec
Coaxial Helium Velocity	0, 0.27, and 2.7 ft/sec

A second series of runs was taken at an axial station 1 inch downstream from the nozzle with a coaxial

*Typical centerline values. Profile data given later provide exact initial condition.

helium flow of 0.27 ft/sec and a variable argon flow between 0.24 and 1.34 gm/sec.

IV. DISCUSSION OF RESULTS

A. Visual Studies

The quantitative results of the visual studies are summarized in Figures 15 and 16, in which the length of the laminar jet is plotted against Reynolds number and velocity, respectively. The region of interest in these figures was originally concentrated on axial locations greater than six inches, because transition to turbulence was not expected to occur much upstream of this location, and the calorimetric probe, which was used to diagnose the jet in the region near the nozzle exit, is a more reliable measurement. This was particularly true in the case of coaxial helium flow, since the high luminosity of the first few inches of the jet precludes precise visual observations.

It is quite apparent from the visual results that the laminar arcjet is very easily disturbed by the coaxial flow, with the laminar jet being shortened to less than six inches at coaxial velocities of only one foot per second. Although some disturbance of the jet by the coaxial flow had been anticipated, it had not been expected that such small velocities would be so significant. This led to closer investigation of the coaxial gas character, and it was observed that the coaxial gas was introduced with considerable initial turbulence, as shown in schlieren photograph of Figure 17.

The quantitative effect of this initial turbulence on producing transition in the laminar jet is discussed later (Section IV-C) in connection with results of the calorimetric probe measurements.

B. Detailed Mapping of Flow Field

Verification of the general nature of the visual study results, as well as quantitative mixing characteristics, were established with the calorimetric probe, covering the region from the nozzle exit plane to the downstream point at which the initial jet had become fully turbulent. Results are summarized in Figures 18 through 21, which show jet centerline values of temperature, velocity, composition, and enthalpy respectively, and in Figures 22 through 27, illustrating radial temperature, velocity, and composition profiles at various axial stations. Also shown on certain of these figures are both theoretical and experimental data on the mixing of a free jet. (The free jet work was performed under the Air Force contract identified previously, but the results reported here are helpful as an aid to the understanding of the duct mixing.)

From the centerline data of Figures 18, 19 and 20, it can be seen that the rapidity of mixing, as evidenced by the rate of decay of the centerline values of temperature, velocity and composition, is strongly influenced by the velocity of the coaxial gas flow, as was indicated by the visual studies discussed above. When the coaxial gas flow was 2.7 ft/sec, mixing was fully accomplished at one inch, or about three jet diameters downstream. At a velocity of 0.27 ft/sec, complete mixing was not accomplished for three inches, or eight diameters downstream.

In the case of no coaxial flow in the duct, as well as in the unbounded jet, mixing was still not completed six inches (about 20 diameters) downstream.

In the case of the free jet, as well as in that for the ducted jet with no coaxial flow (except for Figure 20, which is discussed below), not only did the data indicate confirmation of the visual observations, (i.e., that the jets remained laminar in the region surveyed by the probe) but there was also rather close agreement with laminar mixing theory. These results are in good agreement with studies of laminar mixing of a free arcjet completed recently¹⁰. With the free laminar jet it was found that the flow of helium into the jet was the dominant mechanism for jet cooling and mixing, and that the effects of radiation and ionization were negligible. This experimental result, accurately predicted by the laminar mixing theory, is attributed to helium's high specific heat and high diffusion coefficients at arcjet temperatures. This mechanism was also experimentally indicated in the coaxial studies, and accounts for the similarity between the free and ducted cases at 0.27 ft/sec coaxial flow in the laminar flow region within one or two diameters (1/2 to 1 inch) of the nozzle exit plane.

Direct similarities in this region between the free jet (or the no-coaxial-flow ducted case) and the high-coaxial-flow case (2.7 ft/sec) were, on the other hand, not observed, obviously because of the early transition to turbulence indicated by Figures 15, 18, 19, and 20.

The large difference in helium concentration data between the no-coaxial-flow ducted case and the others, as shown in Figures 20, 22, 23, etc., also has a simple explanation. In this case, the equilibrium concentration of cold helium in the duct is less than 20 per cent (see Figures 22, 23, 24) because most of the helium originally present is very swiftly swept out with the argon jet, and the ambient conditions are therefore substantially different than for the free jet or the higher coaxial-flow ducted cases. On the other hand, helium concentration data for the 0.27 ft/sec ducted coaxial flow, before turbulence is initiated, were found to be essentially similar to those of the free jet case because an ample supply of cold helium was always available at the jet boundary.

Considerable insight into the mechanism of mixing is obtained by consideration of enthalpy rather than temperature decay. Although the various cases differ widely in terms of temperature, velocity and species concentration, a plot of centerline enthalpy (Figure 21) indicates that the basic mixing process is the same in all cases. In this figure, it is shown that the centerline enthalpy decay coincides closely for all coaxial gas flows. Thus it is necessary to conclude that radiation and ionization effects are negligible, since reference to Figure 18 shows that at even small distances from the nozzle, the jet temperatures differ by many thousands of degrees. For example, at one inch from the nozzle, the

temperatures of the jets which were still laminar were about 11,000^oR, while that of the turbulent jet, in which mixing was substantially complete, was only 1,000^oR; still, the enthalpies at the centerline were nearly equal. Clearly, if radiation and ion recombination effects were important mechanisms for jet power loss, the higher-temperature jets should show lower enthalpies. Furthermore, if there were substantial dispersion of the argon jet, the centerline enthalpy of the well-mixed case should be substantially less.

The results of Figure 21 therefore indicate that the principal mechanism for energy transfer (jet cooling) is the inflow of coaxial helium rather than either the direct loss of energy (by radiation or recombination) or the outflow of argon from the core jet.

It may be concluded that while turbulence (of the degree present in these experiments) substantially increases the rate of jet mixing, the effect of the turbulence is to aid the inflow of coaxial helium and not to disperse the argon jet itself.

C. Effects of Turbulence

The very large effect of turbulence on the rate of mixing, in that an apparently small disturbance can cause the jet to lose its initially laminar characteristics, is a prominent result of the experimental program.

Unfortunately, understanding of turbulent jet mixing and the factors causing arcjet turbulence, like all turbulent phenomena, suffers from the fact that present theories of

turbulence are inadequate, and most information on turbulence is empirical. The general character of the observed behavior is consistent with other forms of turbulent-flow experience, however, as is indicated by the summary of results (observed from both the visual and probe studies) in Table I. In this table, Reynolds numbers more than one diameter downstream are based on the length of jet at the point of observation rather than on the jet diameter. The initial Reynolds number (at the nozzle exit) is based on jet diameter, and is 450 for all cases.

Table I shows that transition to turbulent flow did not occur in the free jet until a Reynolds number of 10,000 was reached, while very small disturbances, such as convective currents resulting from the simple presence of the duct* or from very small coaxial flows, caused transition at Reynolds numbers of 4,000 and 3,000 respectively. Furthermore, a coaxial flow of only 2.7 feet per second of helium produced transition in less than one jet diameter from the exit plane at a Reynolds number of only 450.

*The convective turbulence caused simply by the presence of the duct was evidenced by visually-observed motion of dust particles, and has also been observed in combustion experiments where the flow conditions were similar.¹¹

TABLE I

Effect of Test Conditions on Reynolds Number at Transition

<u>TEST CONDITIONS</u>	<u>APPROXIMATE LAMINAR JET LENGTH, INCHES</u>	<u>APPROXIMATE REYNOLDS NUMBER AT TRANSITION</u>
Free jet, 1 atm, no coaxial flow	18	10,000
Ducted jet, 1 atm, no coaxial flow	5	4,000
Ducted jet, 1/5 atm, no coaxial flow	18	4,000
Ducted jet, 1 atm, 0.27 ft/sec coaxial He	2	3,000
Ducted jet, 1 atm, 2.7 ft/sec coaxial He	1/2	450

It should be remarked that only by basing the Reynolds number on a linear dimensional quantity can transition data be obtained which are consistent with the general range in which it is usually observed. Reynolds numbers based on the jet diameter remained nearly constant at about 500 for all types of flow observed, and therefore are not useful as a guide to transition predictions.

On the basis of the above results, it is believed that in any practical propulsion device it would be impossible to maintain laminar flow for more than a few nozzle diameters. These devices should therefore be designed to operate in the turbulent mode.

D. Variation of Mass Flow in Core Jet

Figures 27 through 29 are profiles of temperature, velocity, and composition respectively at one inch downstream from the nozzle exit plane when the argon jet mass flow was varied from 0.24 to 1.34 g/sec while the coaxial helium flow was maintained at 0.27 ft/sec. It can be concluded from the general shape of the profiles that spreading and mixing were little affected, although a wide variation of mass flow was experienced. The plasma generator efficiency is significantly augmented by increased mass flows, and this results in the higher temperatures and velocities observed at the high mass flows. The plots do not indicate which profiles represent laminar flows and which represent turbulent flows, but based on visual observations the profiles at the higher mass flows are likely to be turbulent. It is a tentative conclusion, which must be examined by additional work, that high mass flow rates tend to reduce jet mixing over a given distance, even though turbulence may be present. This is, of course, similar to the phenomena observed in more familiar types of jets.

V. CONCLUSIONS

1. Up to about three jet diameters downstream from the nozzle exit plane there is little difference between the experimental laminar mixing characteristics of a free jet and a bounded jet when the coaxial flow of helium in the duct is sufficient to provide similar ambient helium con-

centrations, but not so large as to disturb the laminar character of the jet. In this region a theoretical analysis for a laminar free jet is also applicable to a similar ducted jet.

2. Very low velocities of an initially turbulent coaxial flow were sufficient to cause transition in an initially laminar core jet, and increases in coaxial gas velocities produced earlier transition to turbulence.

3. Mixing of the jet was very rapid once turbulence was initiated, and in one case (the highest coaxial velocity tested) complete mixing of the jet was accomplished in less than three jet diameters from the nozzle exit.

4. With increased core-jet mass flow, mixing of the jet at three diameters downstream was diminished, even though the jet may have become turbulent. This is, of course, similar to the phenomena observed in more familiar types of jets.

5. The most significant process in the mixing of either a free or a ducted laminar argon arcjet was found to be the flow of helium into the jet, the effects of radiation and ionization being negligible. This behavior results from helium's high specific heat and high diffusion coefficient at arcjet temperatures. The principal effect of turbulence, in the scale studied in the present experiments, was to cause augmentation of the helium inflow rather than dispersion of the jet.

6. An arcjet Reynolds number based on length rather than diameter was most useful in correlating the onset of turbulence, in accordance with conventional laminar free-jet practice.

7. Owing to the difficulty of obtaining and maintaining stable laminar jets, turbulent models should be used in the design of practical propulsion devices.

8. The results indicate potential feasibility of the coaxial flow, gaseous-core nuclear rocket concept, since it was found that the argon arcjet decayed as a result of inflow of cool coaxial helium rather than dispersion of the argon core, even when turbulent mixing was significant. Before this conclusion can be applied to the coaxial gaseous-core rocket, however, it will be necessary to examine the mixing mechanism for coaxial gas velocities up to one or more orders of magnitude greater than the core jet velocity. This study is planned under a subsequent NASA contract.

REFERENCES

1. NASA Contract NAS 3-3680 with Princeton University, dated 1 May 1963.
2. Weinstein, H., and Ragsdale, R. G., "A Coaxial-Flow Reactor -- A Gaseous Nuclear-Rocket Concept," ARS Preprint No. 1518-60, November, 1960.
3. Weinstein, H., and Todd, C. A., "A Numerical Solution of the Problem of Mixing of Laminar Coaxial Streams of Greatly Different Densities -- Isothermal Case," NASA TN D-1534, 1963.
4. Ragsdale, R. G., and Weinstein, H., "On the Hydrodynamics of a Coaxial Flow Gaseous Reactor," Proc. ARS/ANS/IAS Nuclear Propulsion Conference, August 1962, AEC TID 7653, Part I, pp. 82-88.
5. Ragsdale, R. G., Weinstein, H., and Lanzo, C. D., "Correlation of a Turbulent Air-Bromine Coaxial-Flow Experiment," NASA TN D-2121, February, 1964.
6. Grey, J., Jacobs, P. F., and Sherman, M. P., "Calorimetric Probe for the Measurement of Extremely High Temperature," Rev. Sci. Instr. 33, July 1962, pp. 738-741.
7. Grey, J., Sherman, M. P., and Jacobs, P. F., "Measurements of Arcjet Radiation with a Cooled Collimated Probe," IEEE Transactions on Nuclear Science, Vol. NS-11, January 1964, p. 176.
8. Grey, J., and Jacobs, P. F., "Experiments on Turbulent Mixing in a Partly-Ionized Gas," AIAA Journal 2, March 1964, p. 433.
9. Grey, J., Williams, P. M., Sherman, M. P., and Jacobs, P. F., "Laminar Mixing and Heat Transfer Phenomena Between a Partially-Ionized Gas and a Gaseous Coolant," Report No. ARL 63-237, OAR, USAF, December 1963.
10. Sherman, M. P., and Grey, J., "Interactions Between a Partly-Ionized Laminar Subsonic Jet and a Cool Stagnant Gas", Princeton University Aeronautical Engineering Laboratory, Report No. 707, September 1964.
11. Becker, H. A., Hottel, H. C., and Williams, G. C., Ninth Symposium (International) on Combustion, p. 7, Academic Press 1963.

- KEY
T. TEMPERATURE
P. PRESSURE
m. MASS FLOW RATE
k. THERMAL CONDUCTIVITY
V. VOLTAGE
A. CURRENT

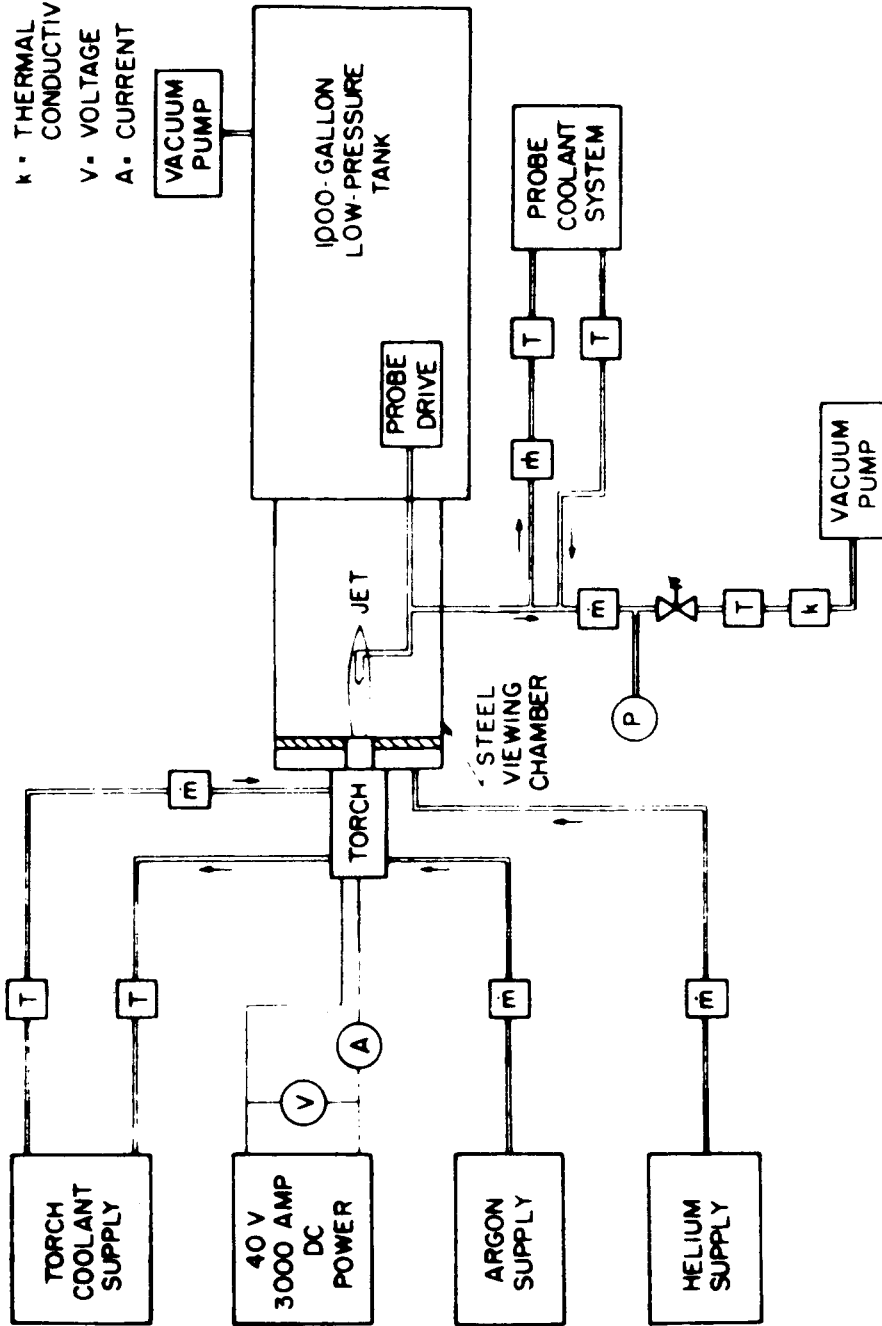
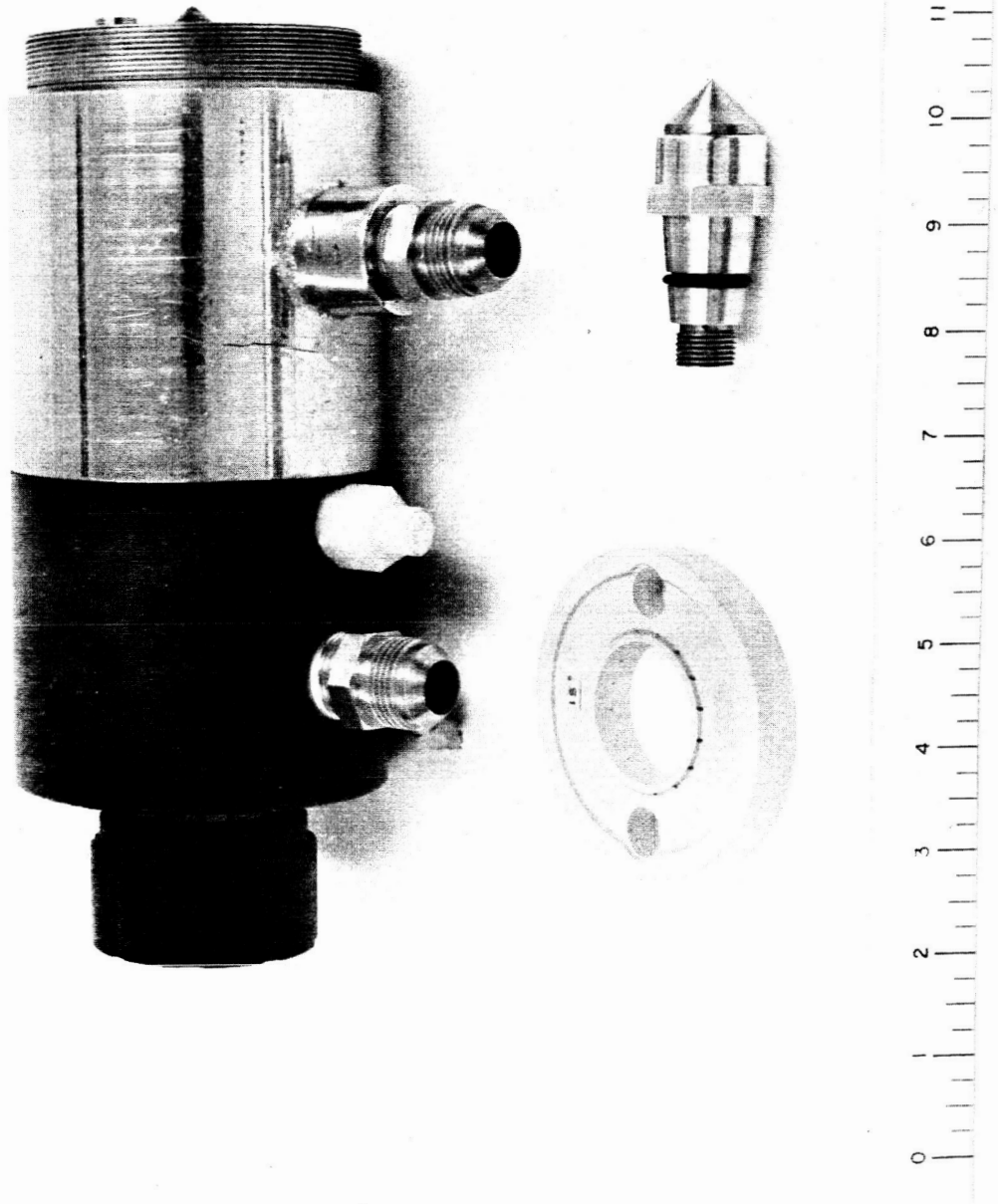


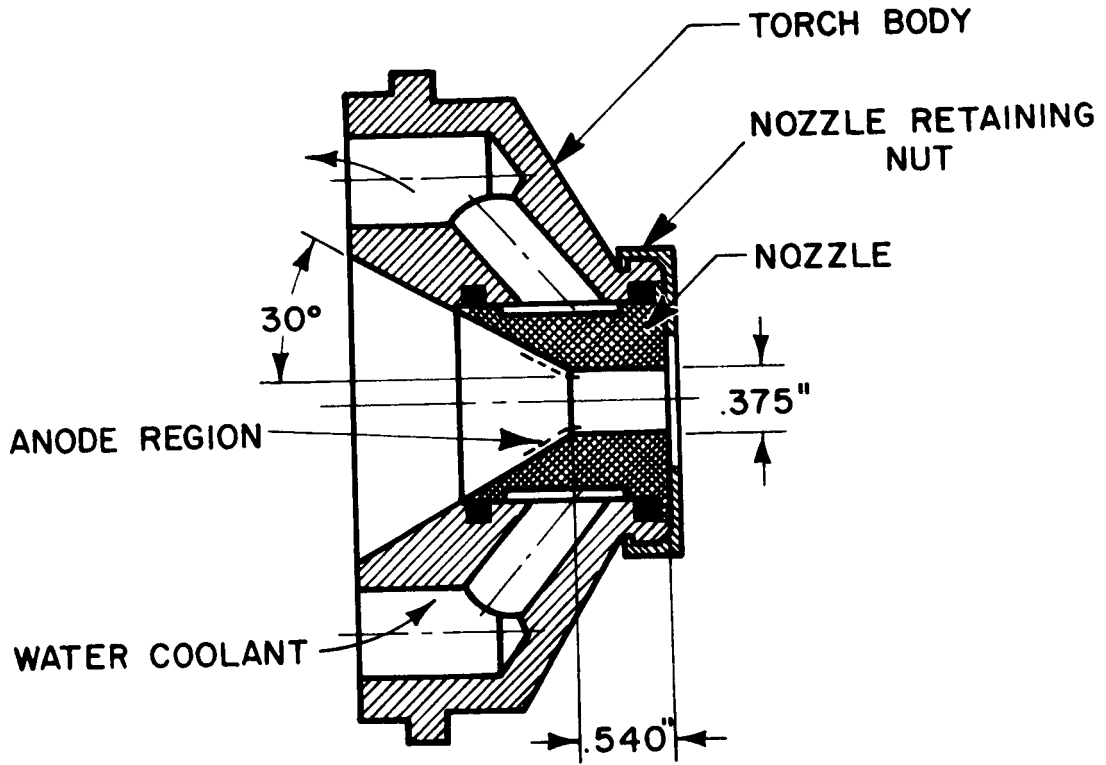
DIAGRAM OF APPARATUS

FIGURE 1



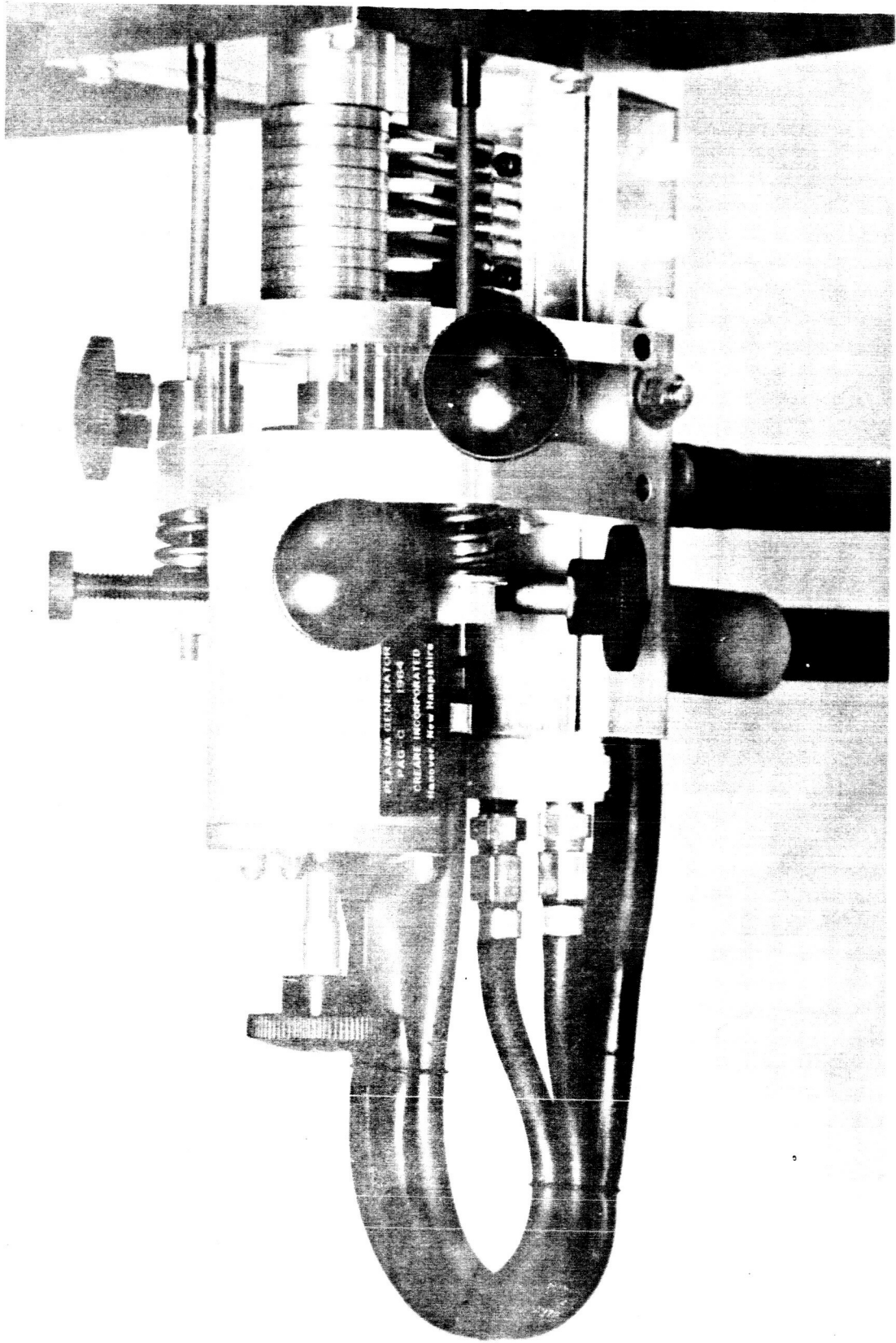
THERMAL DYNAMICS F-80 ARCJET TORCH WITH SWIRL PLATE AND CATHODE

FIGURE 2



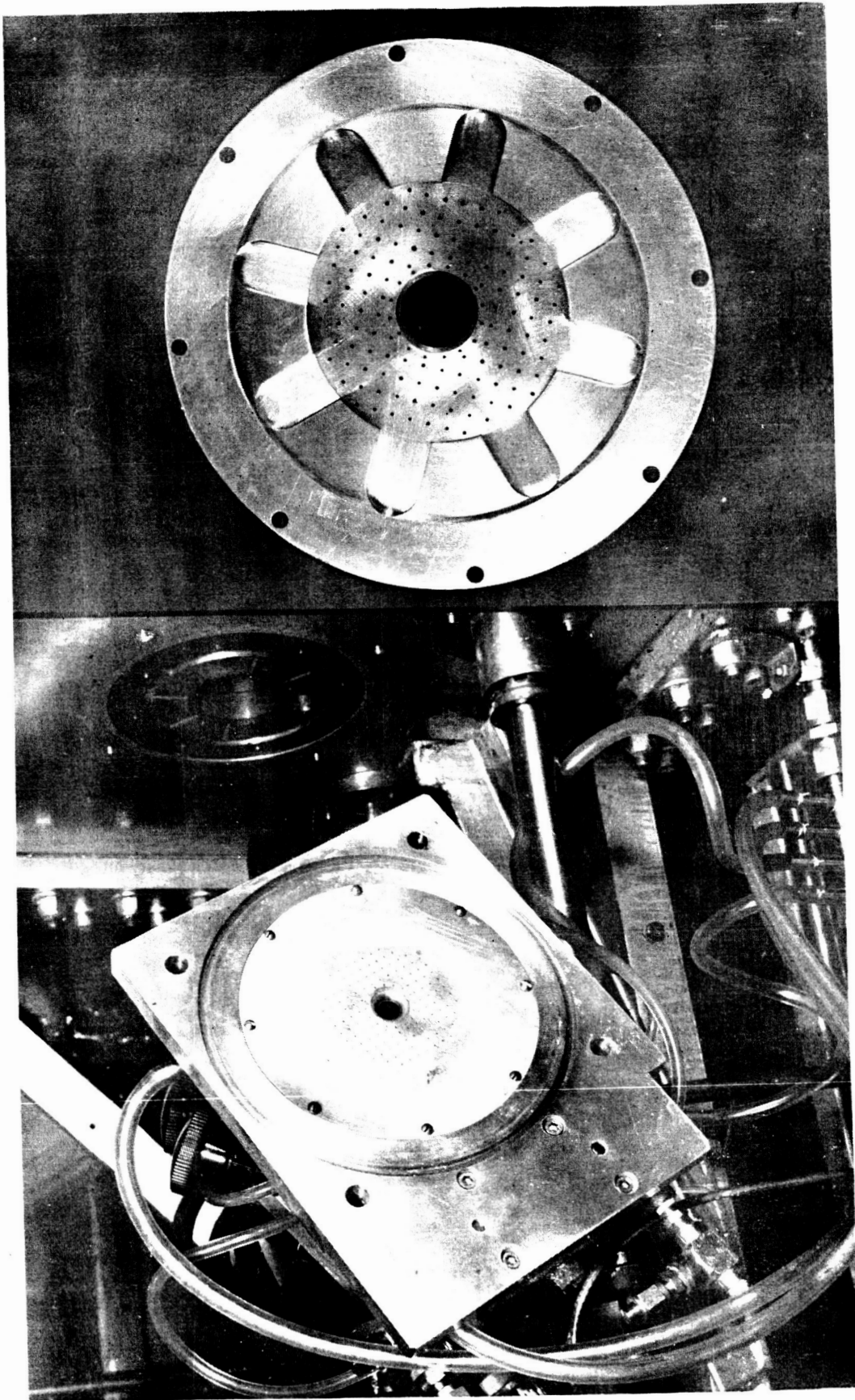
NOZZLE - ANODE USED WITH F-80
ARCJET TORCH

FIGURE 3



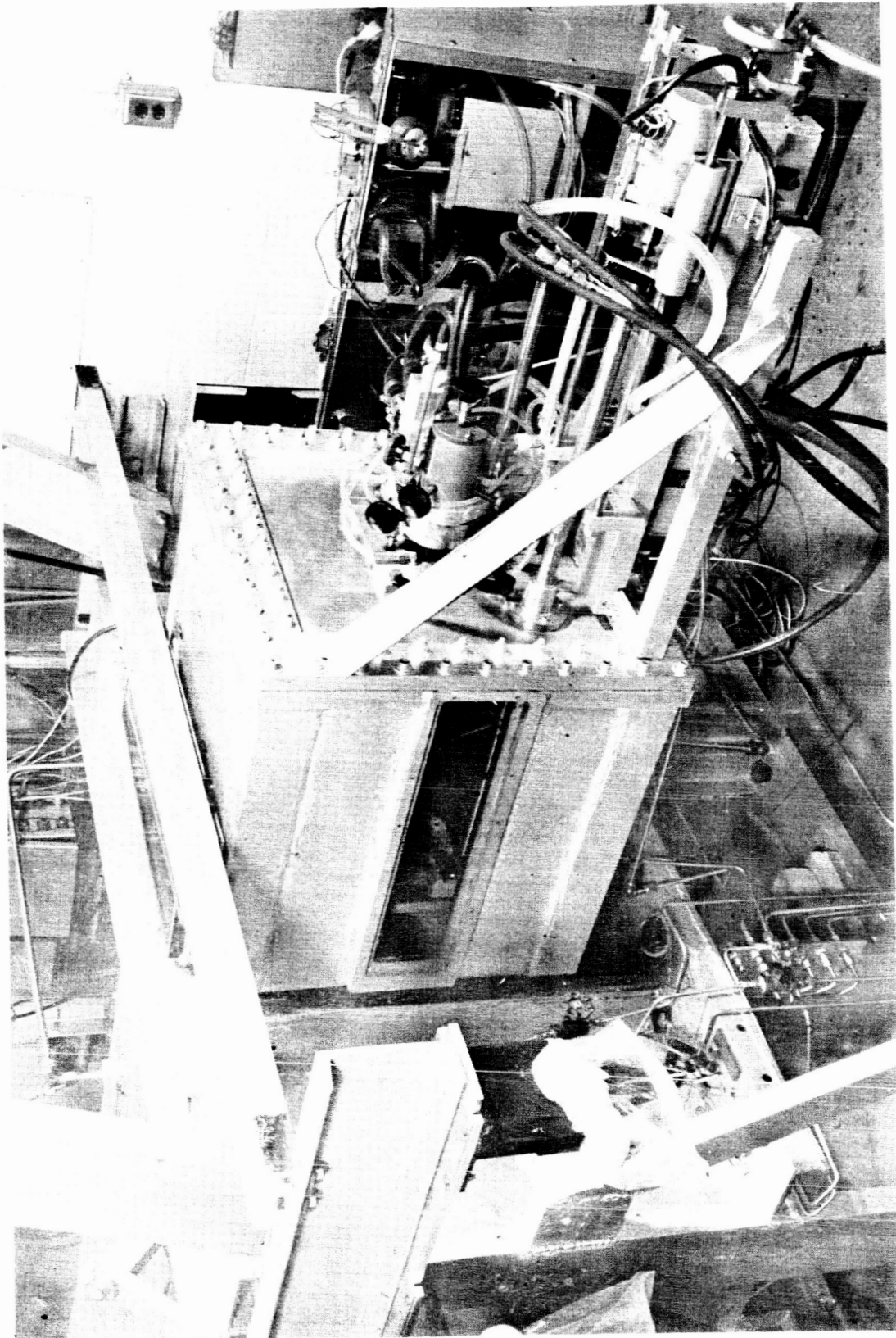
CREARE PLASMA GENERATOR

FIGURE 4



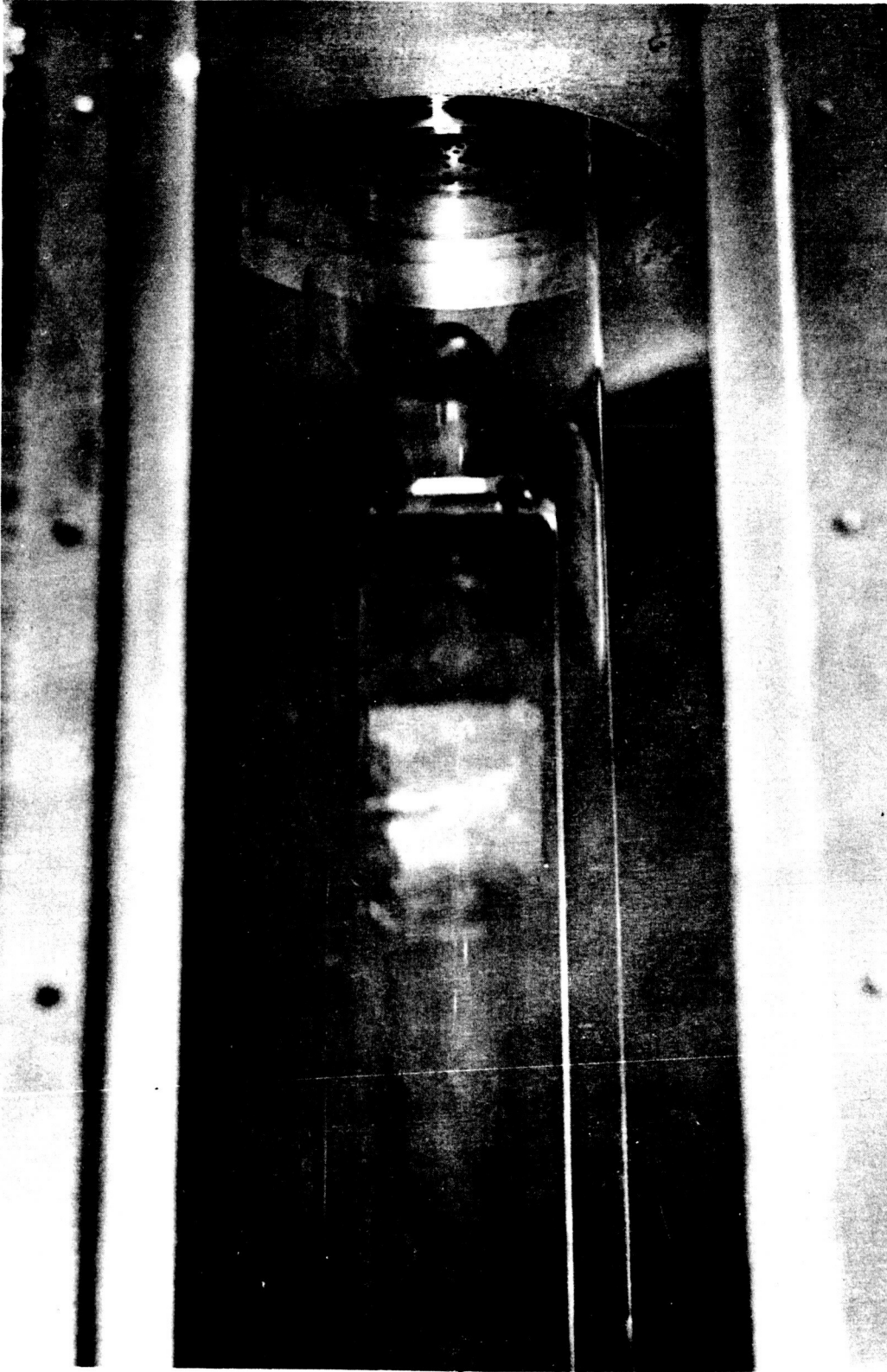
ADAPTER AND LIGHT GAS INJECTION PLATE

FIGURE 5



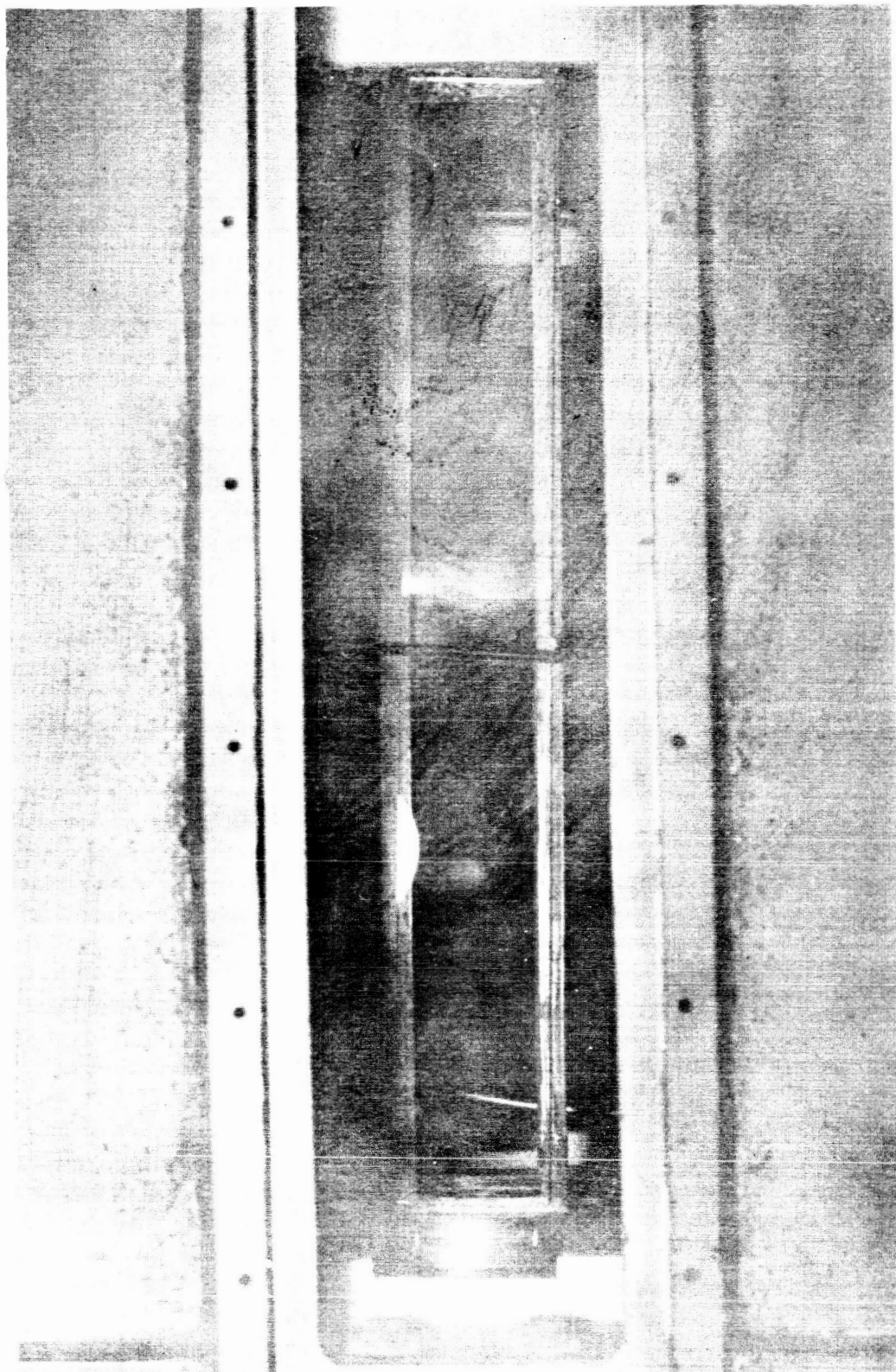
CREARE GENERATOR INSTALLED IN TEST APPARATUS

FIGURE 6



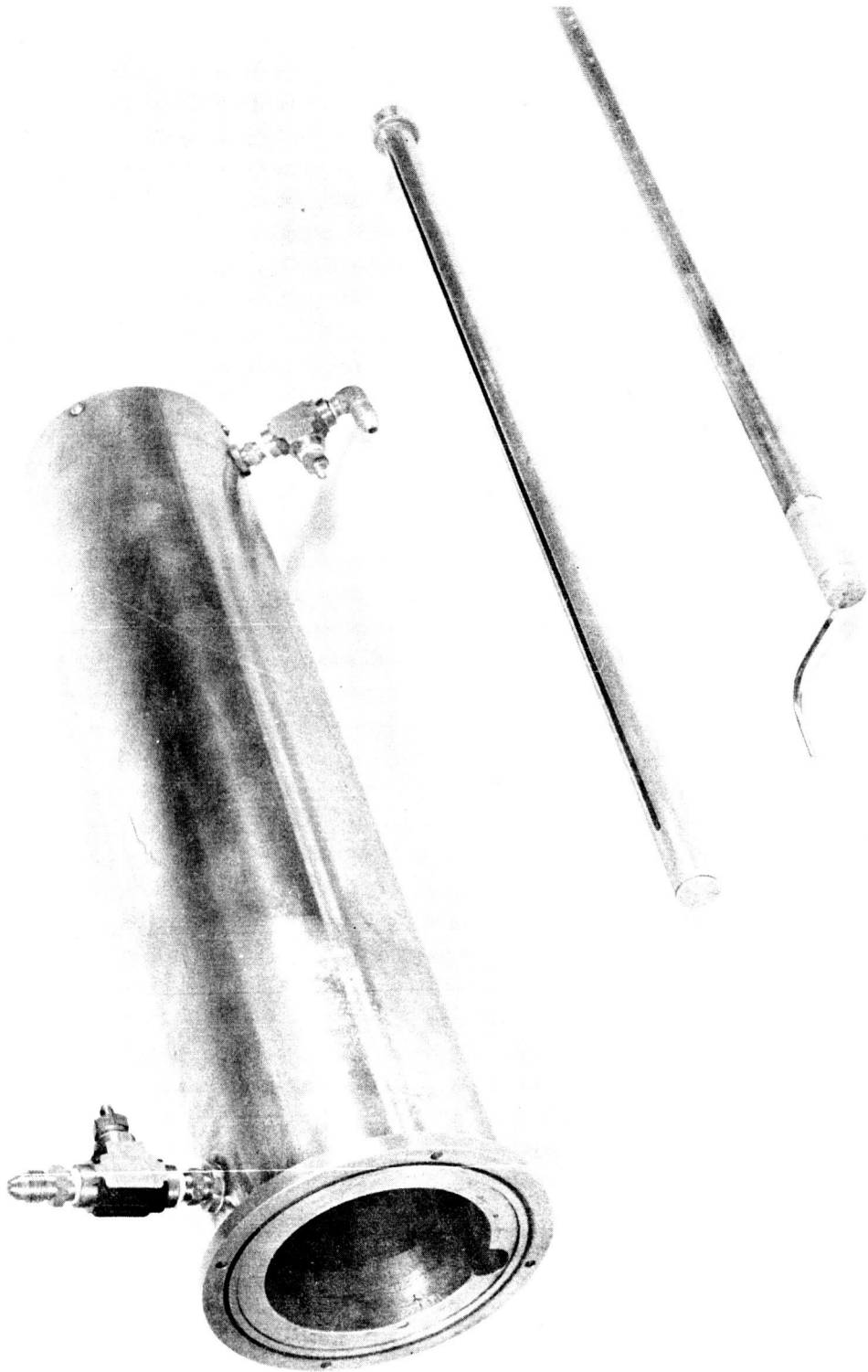
VIEW OF ROUND VYCOR DUCT USED FOR VISUAL
COAXIAL-FLOW TRANSITION STUDIES

FIGURE 7



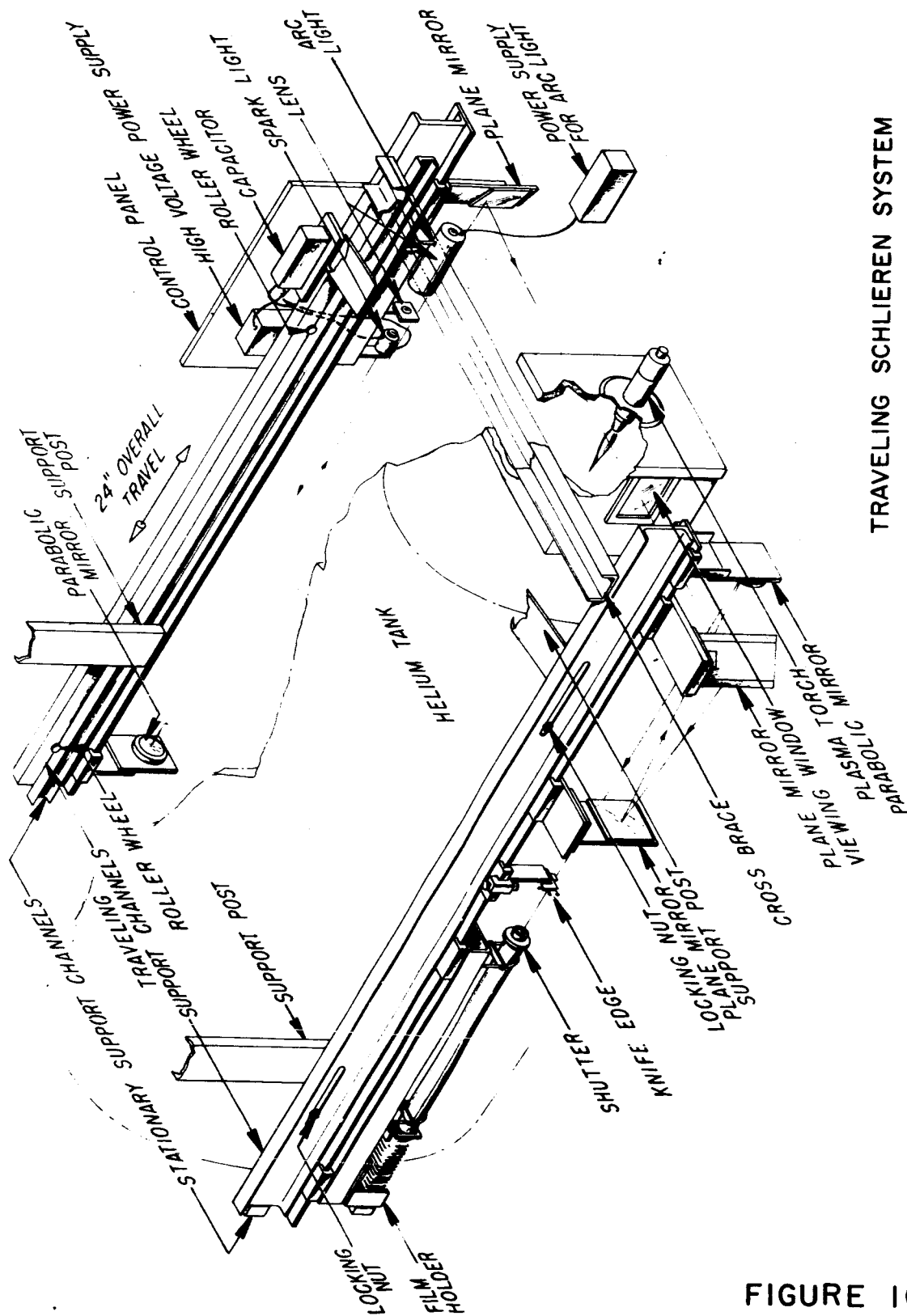
VIEW OF SQUARE DUCT USED FOR COAXIAL-FLOW
TRANSITION STUDIES BY SCHLIEREN PHOTOGRAPHY

FIGURE 8



VIEW OF CALORIMETRIC DUCT USED FOR DETAILED
COAXIAL - FLOW MIXING AND HEAT TRANSFER MEASUREMENTS

FIGURE 9



TRAVELING SCHLIEREN SYSTEM

FIGURE 10

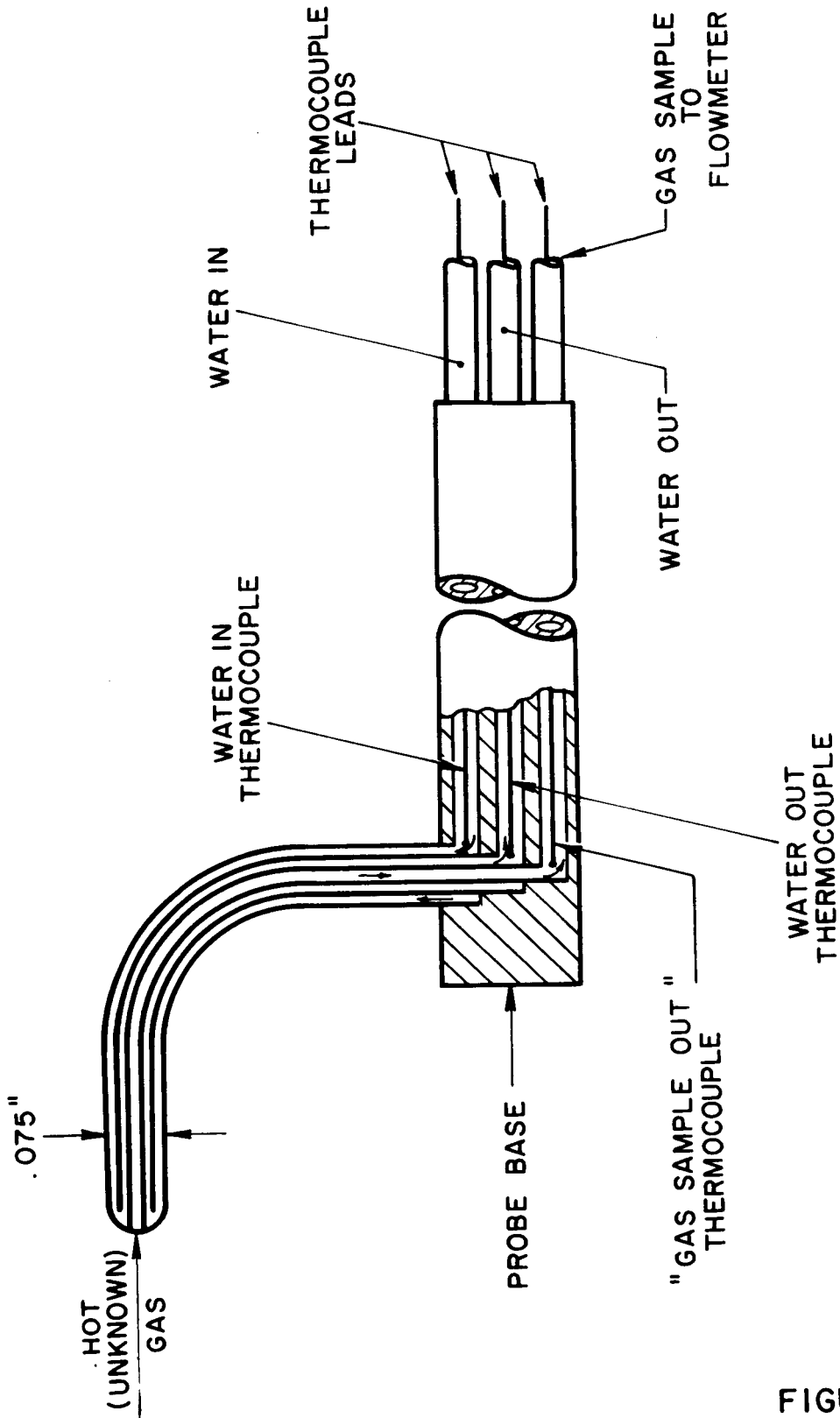
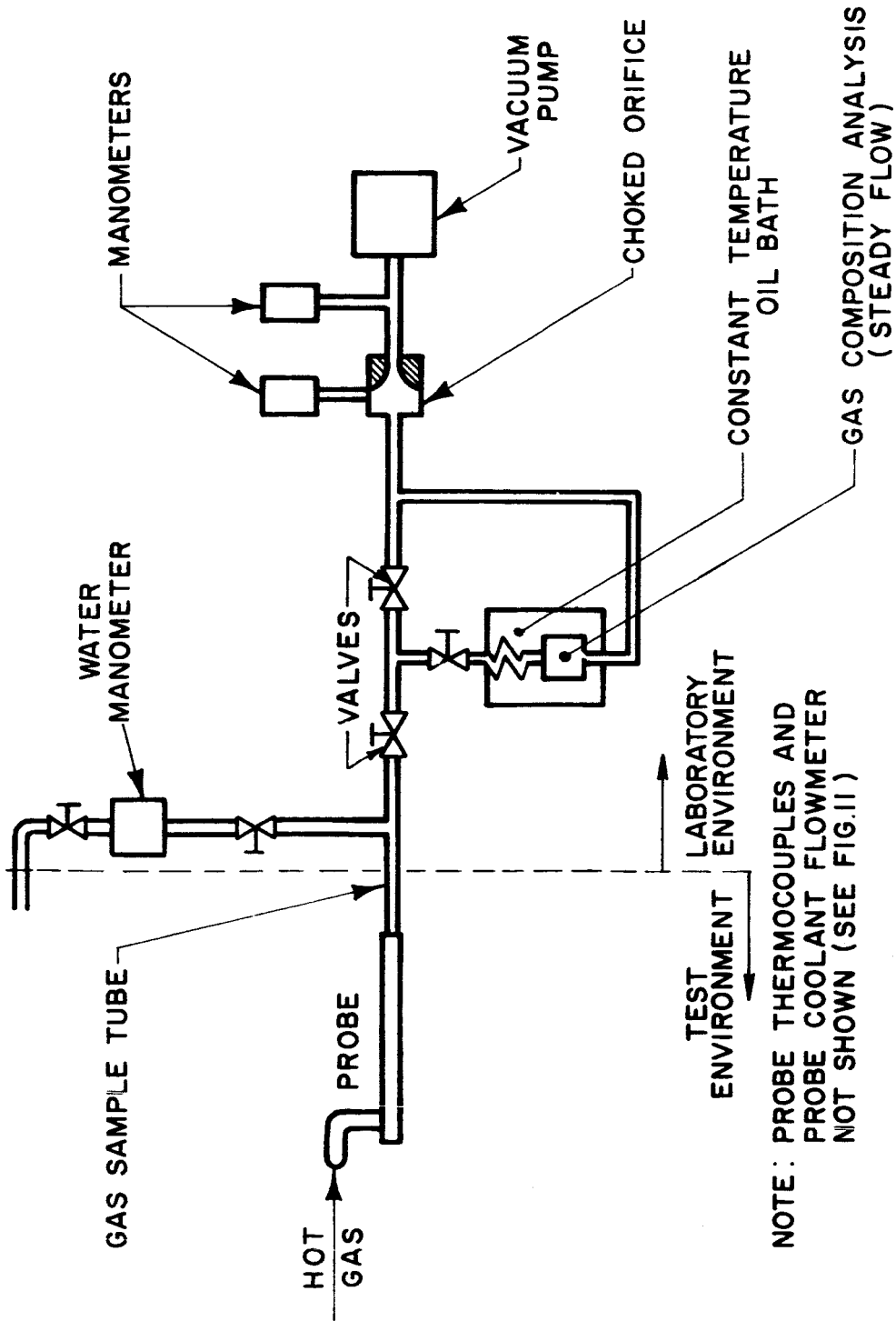


DIAGRAM OF CALORIMETRIC PROBE

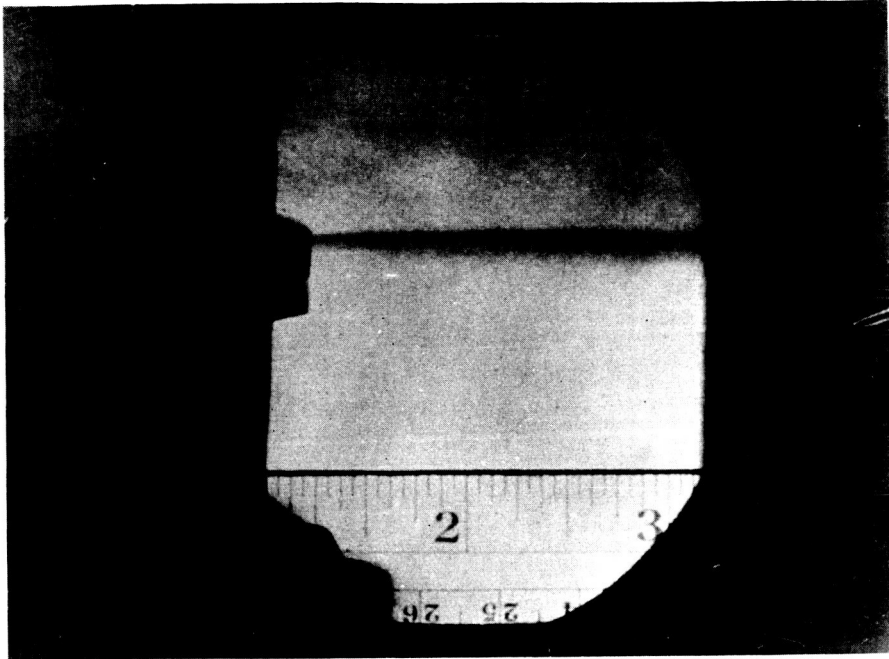
FIGURE II



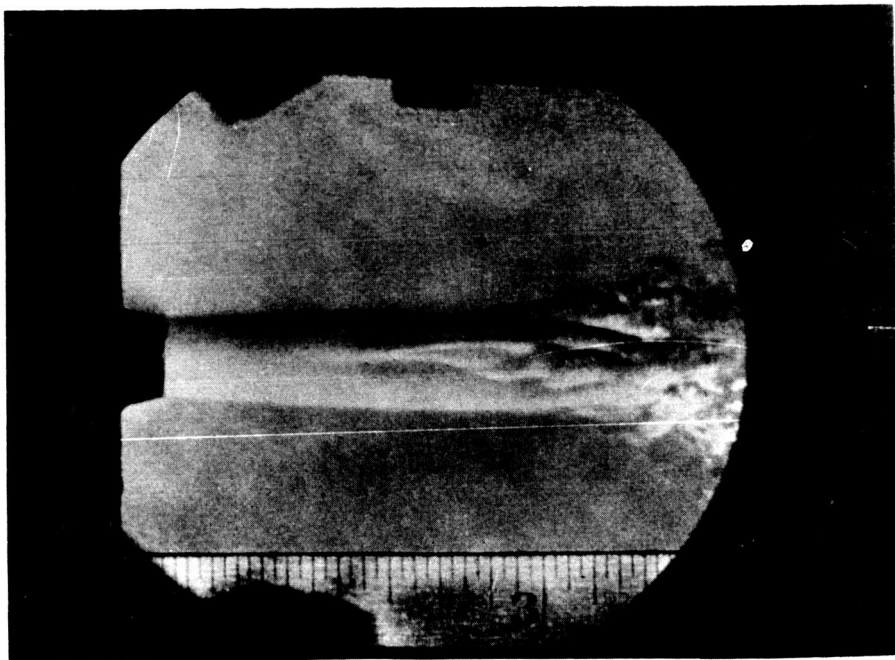
NOTE: PROBE THERMOCOUPLES AND
PROBE COOLANT FLOWMETER
NOT SHOWN (SEE FIG.11)

DIAGRAM OF INSTRUMENTATION USED WITH TARE-MEASUREMENT
CALORIMETRIC PROBE TO MEASURE ENTHALPY, VELOCITY
AND GAS COMPOSITION

FIGURE 12



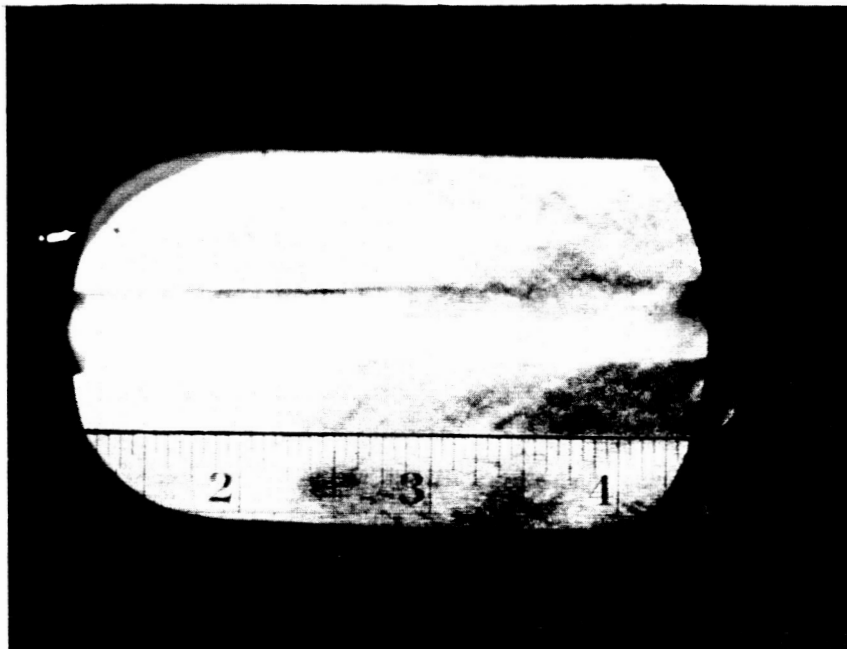
LAMINAR



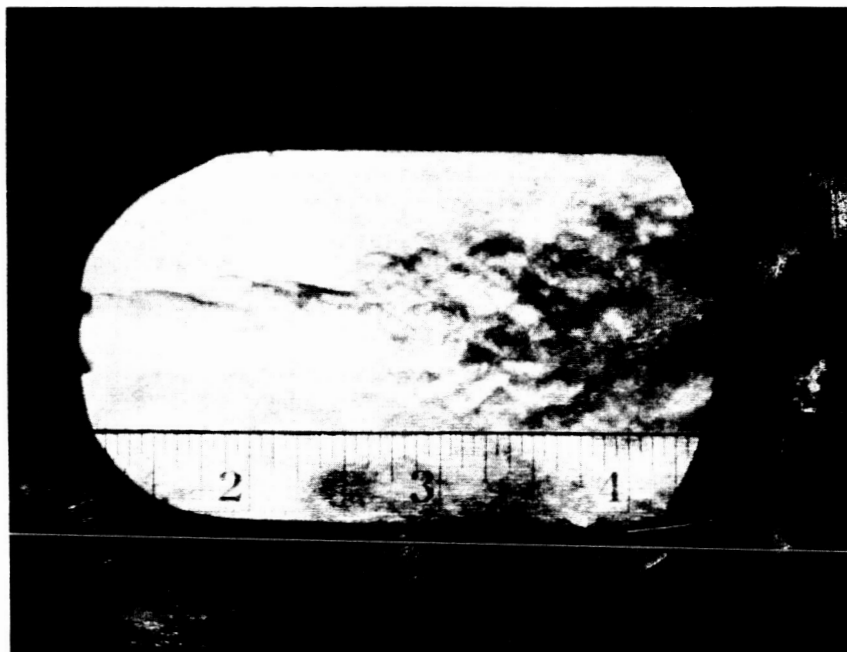
LAMINAR AND TRANSITION

SCHLIEREN PHOTOGRAPHS OF A FREE ARGON
ARCJET IN NITROGEN

FIGURE 13



LAMINAR



TURBULENT

SCHLIEREN PHOTOGRAPHS OF ARGON ARCJET
IN NITROGEN IN 3 INCH SQUARE DUCT
(3/8" DIAMETER NOZZLE - 1 ATMOSPHERE)

FIGURE 14

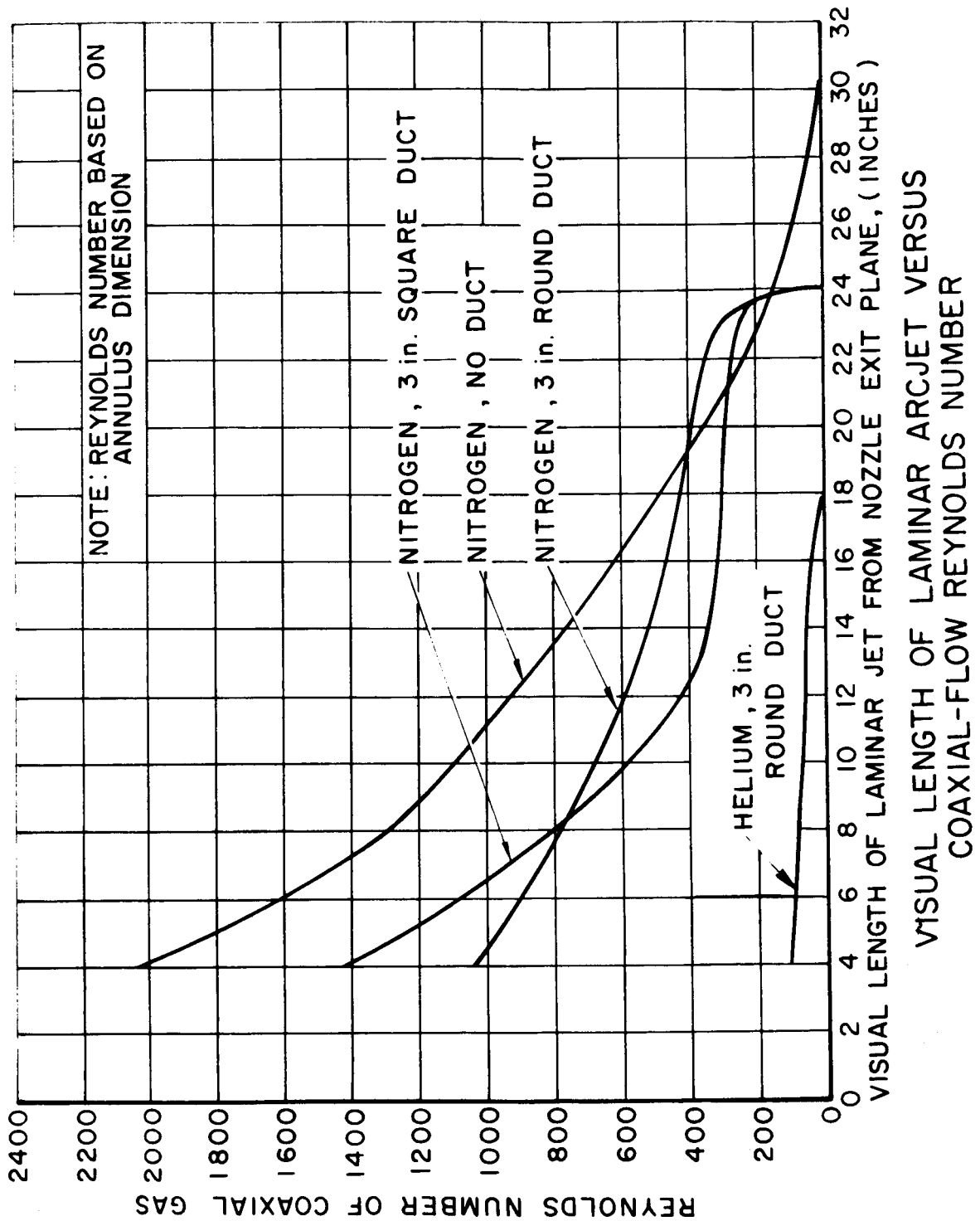
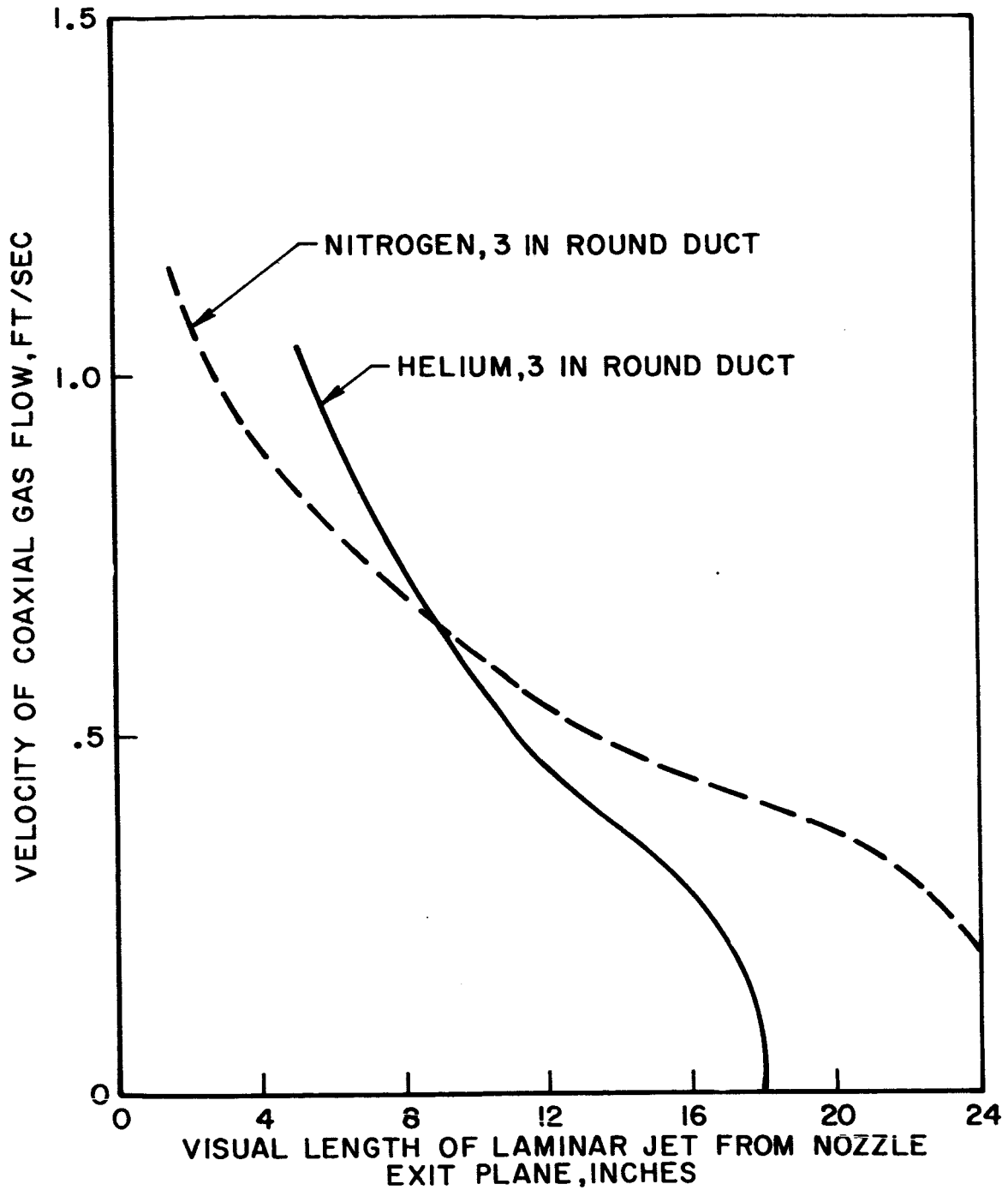


FIGURE 15

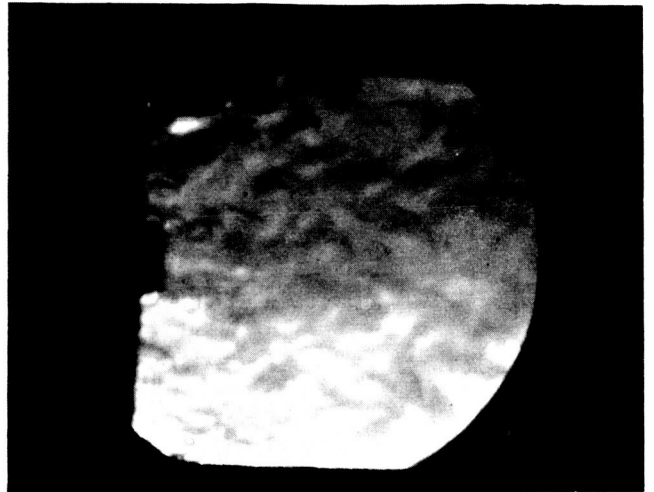


VISUAL LENGTH OF LAMINAR ARCJET
VERSUS COAXIAL-FLOW VELOCITY

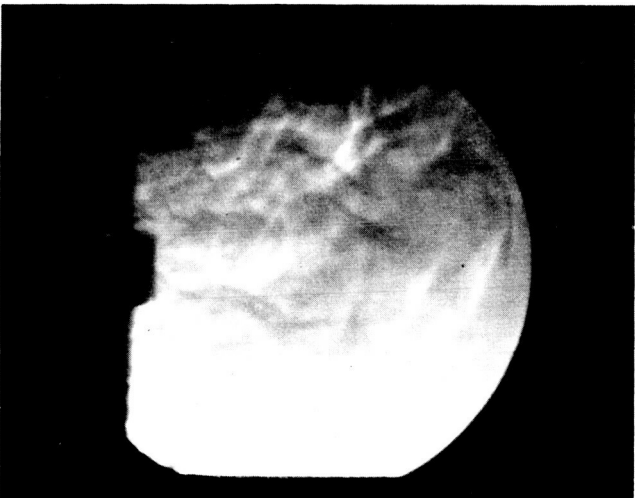
FIGURE 16



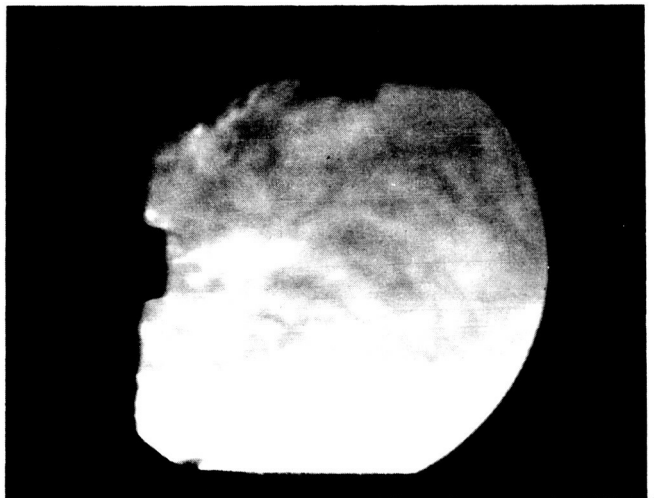
NO INJECTION PLATES



COARSE PERFORATED PLATE



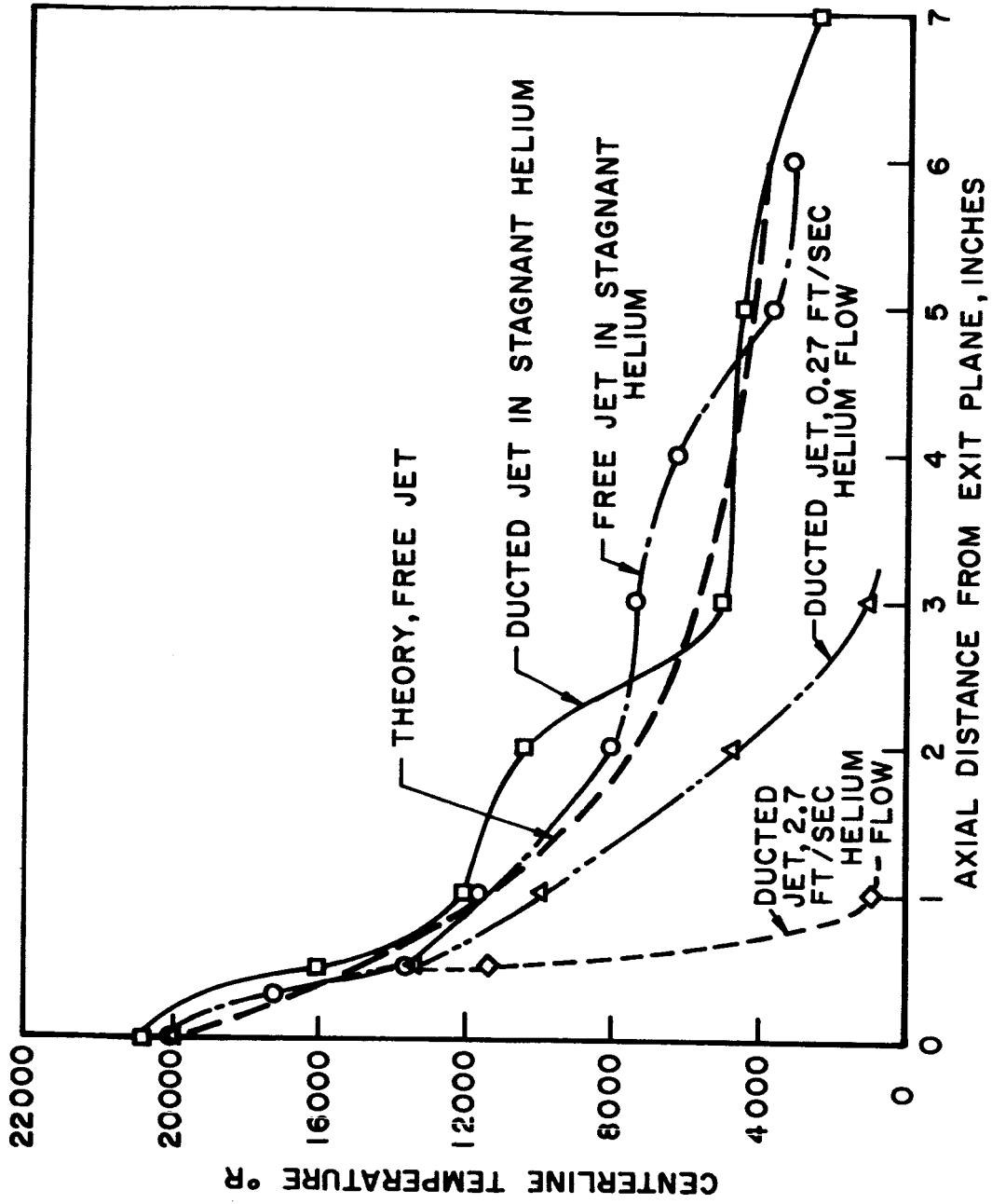
**COARSE AND MEDIUM
PERFORATED PLATES**



**COARSE AND MEDIUM
PERFORATED PLATES
AND 100 MESH SCREEN**

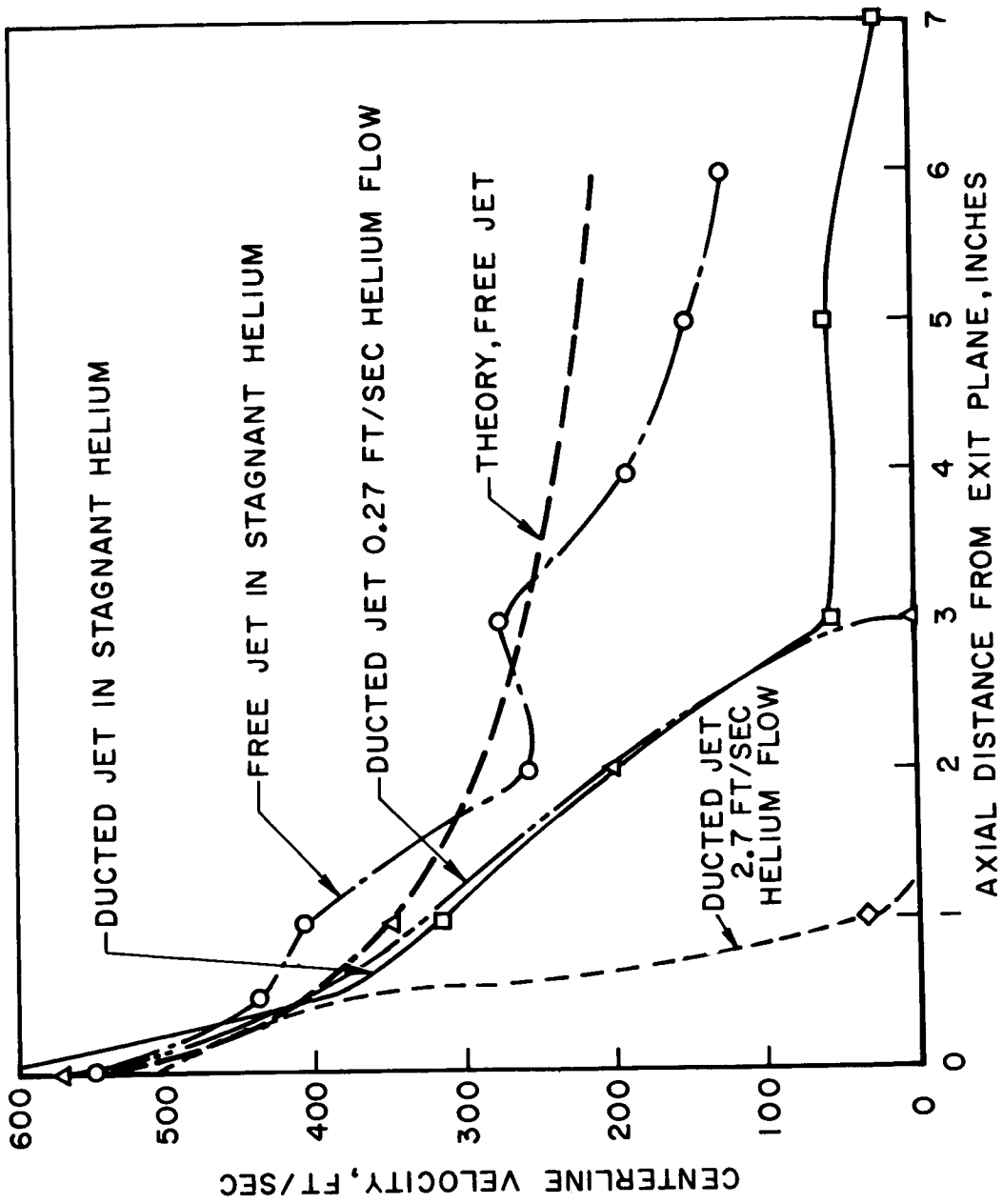
**SCHLIEREN PHOTOGRAPHS SHOWING SCALE OF TURBULANCE
IN COAXIAL HELIUM FLOW
(HELIUM VELOCITY 0.6 FT/SEC)**

FIGURE 17



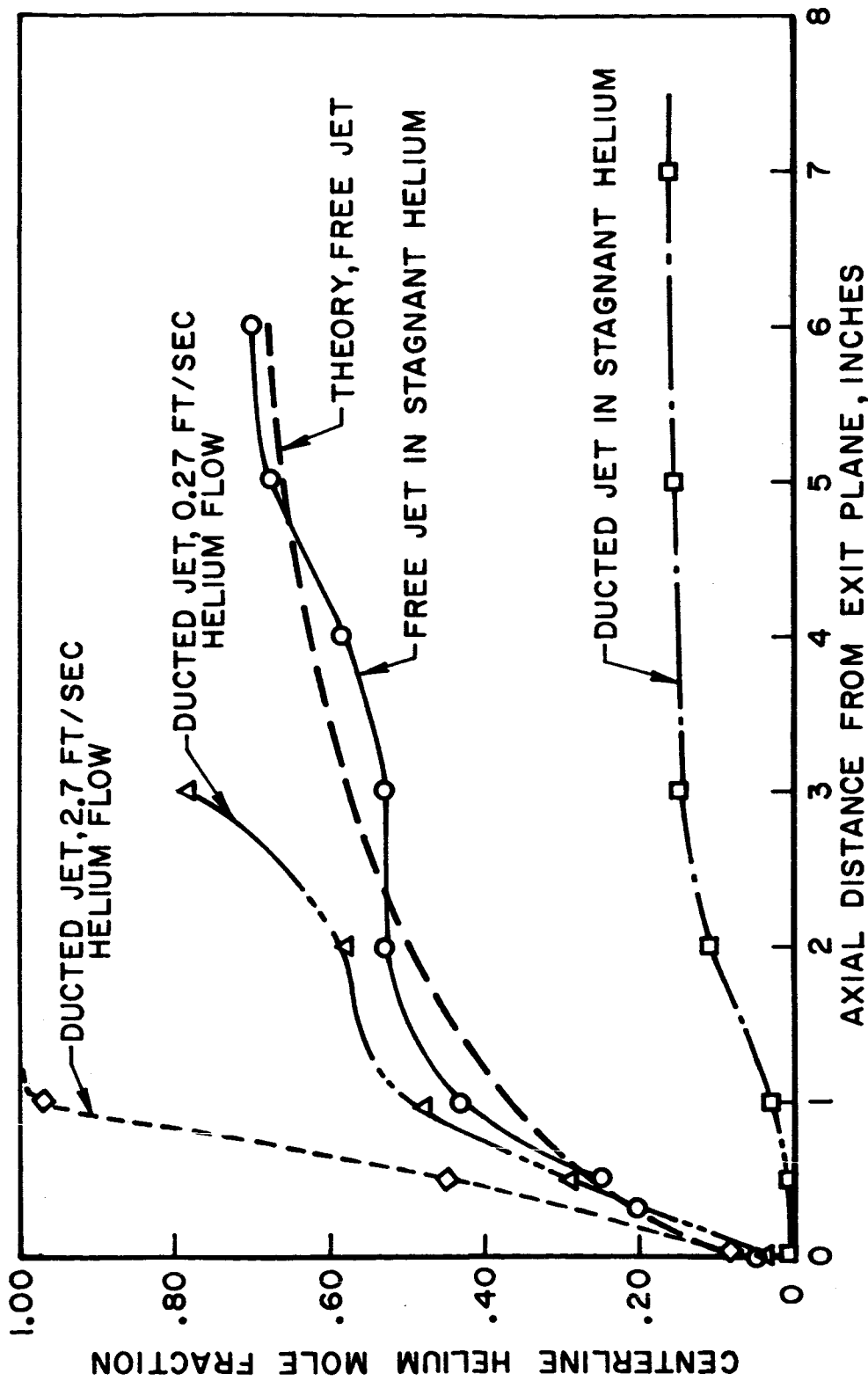
CENTERLINE TEMPERATURES VERSUS AXIAL POSITION

FIGURE 18



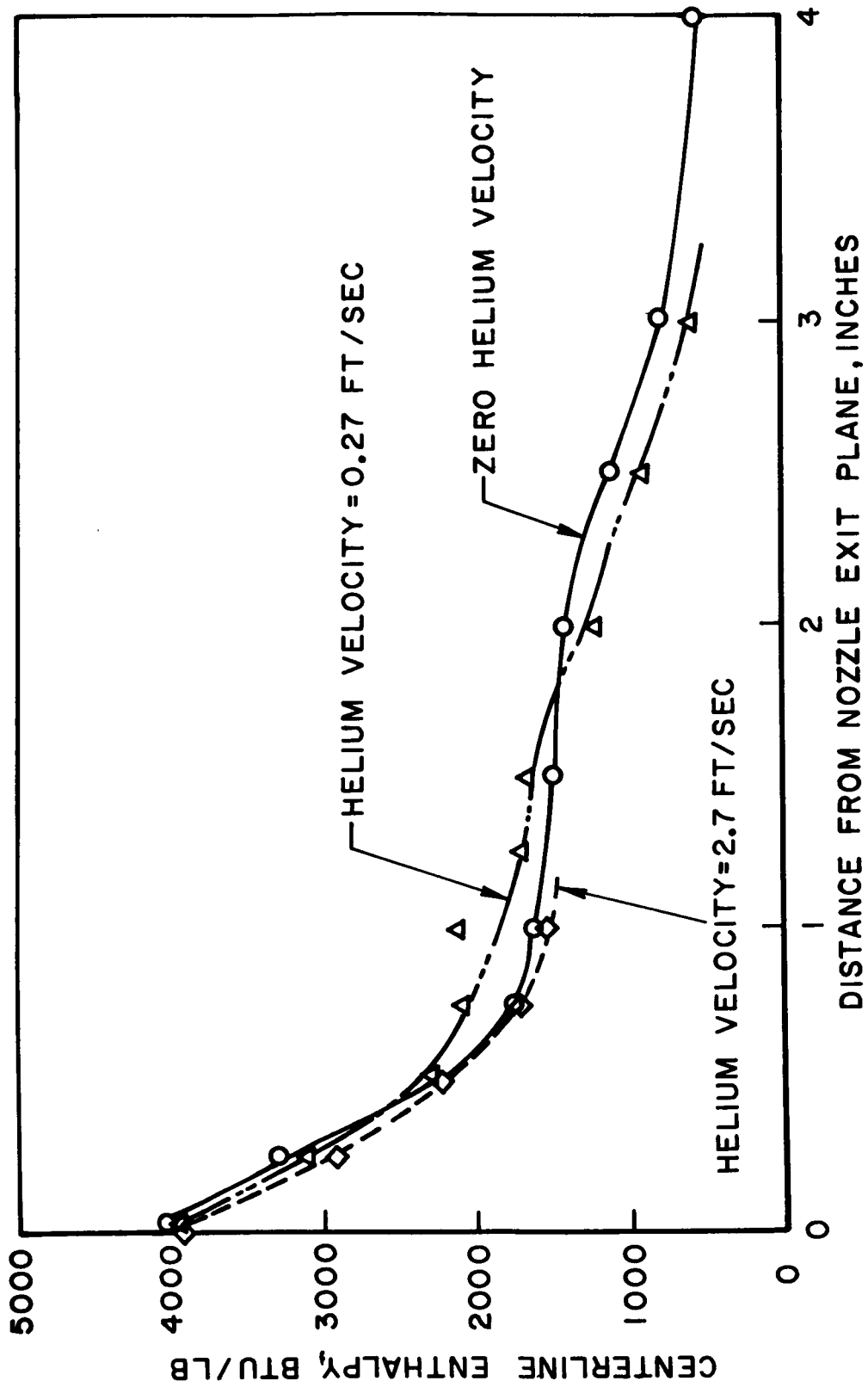
CENTERLINE VELOCITIES VERSUS AXIAL POSITION

FIGURE 19



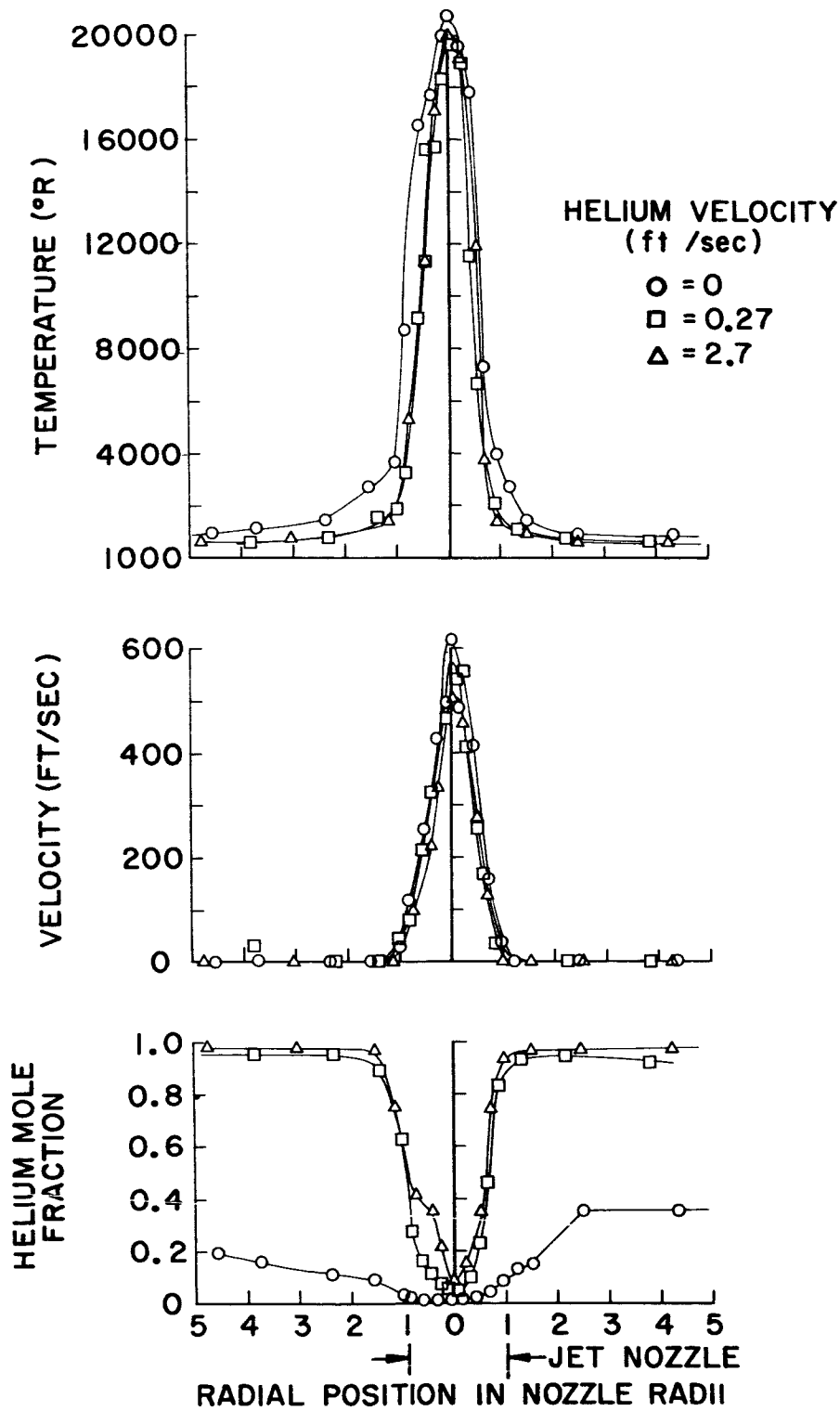
CENTERLINE HELIUM CONCENTRATION VERSUS AXIAL POSITION

FIGURE 20



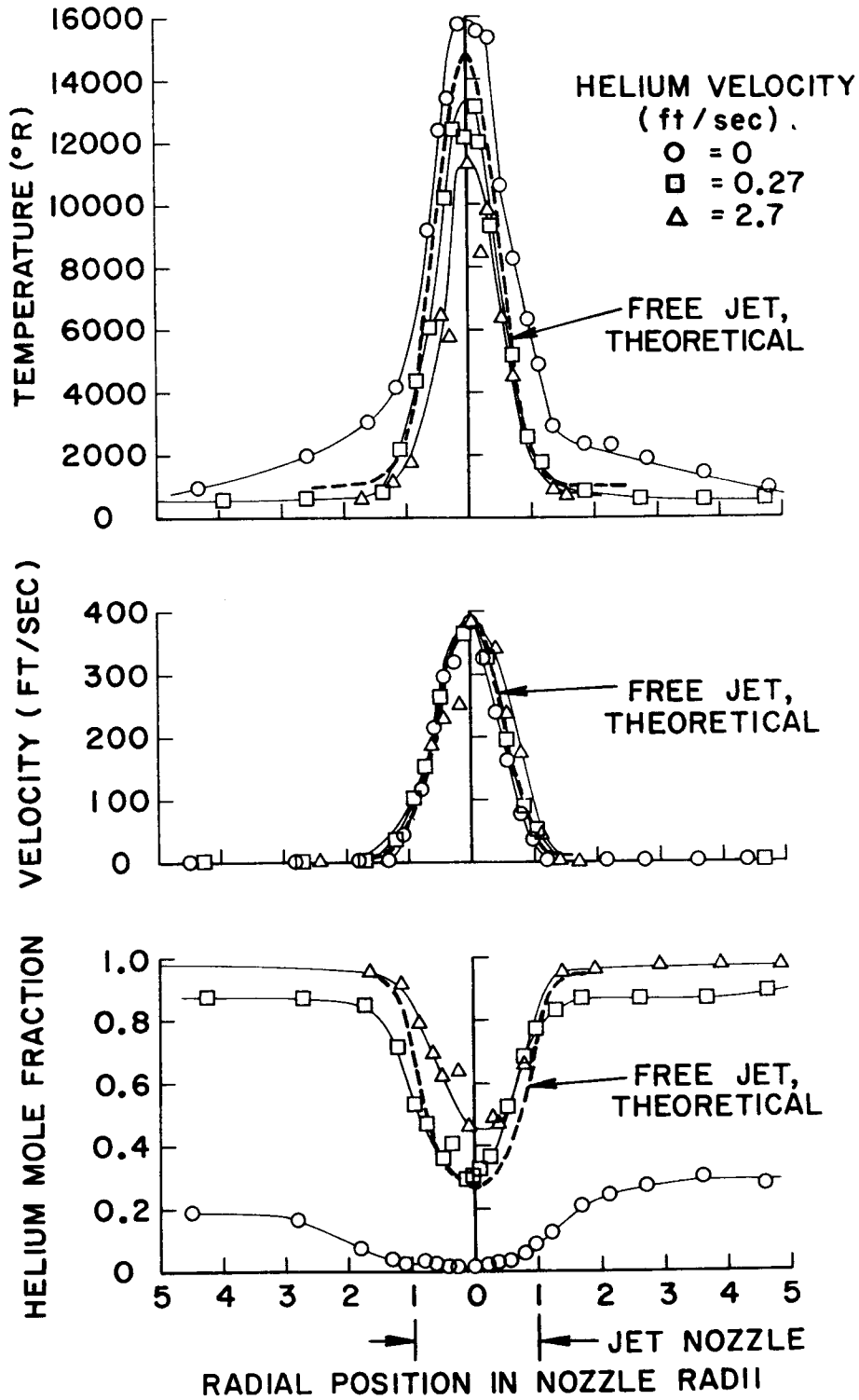
CENTERLINE ENTHALPY VERSUS AXIAL POSITION

FIGURE 21



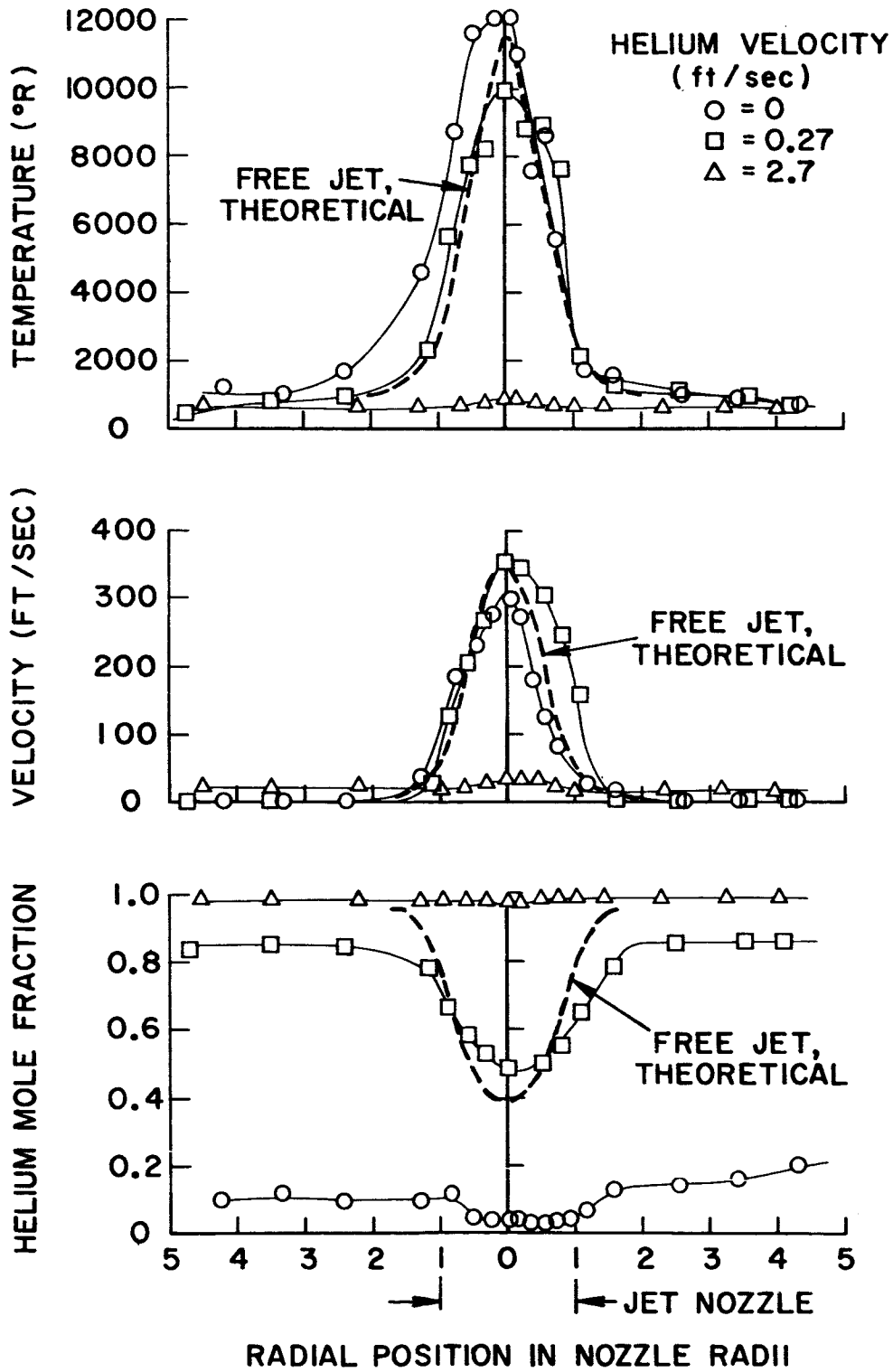
TEMPERATURE, VELOCITY AND COMPOSITION PROFILES AT NOZZLE EXIT PLANE

FIGURE 22



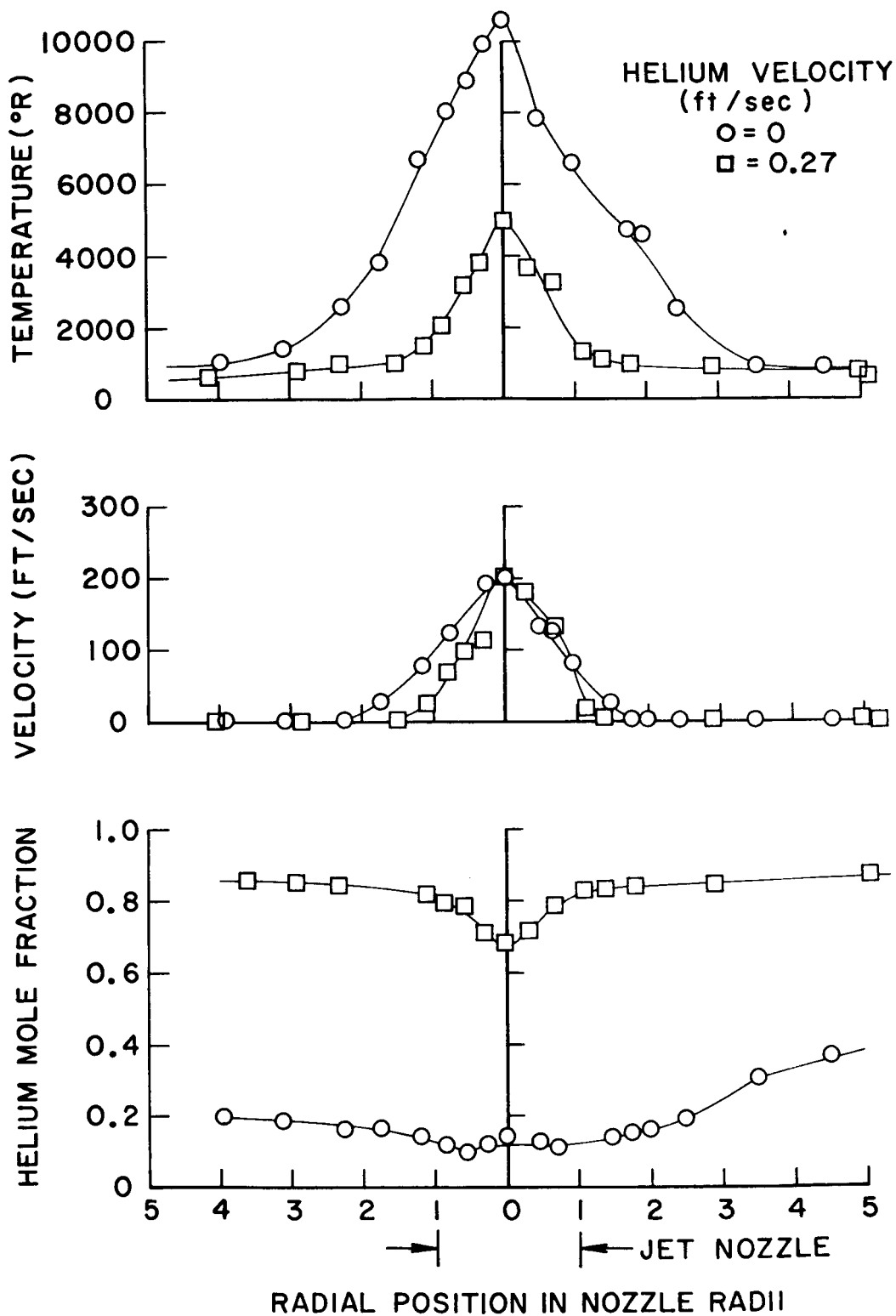
TEMPERATURE, VELOCITY AND COMPOSITION PROFILES AT 1/2 INCH DOWNSTREAM FROM NOZZLE EXIT PLANE

FIGURE 23



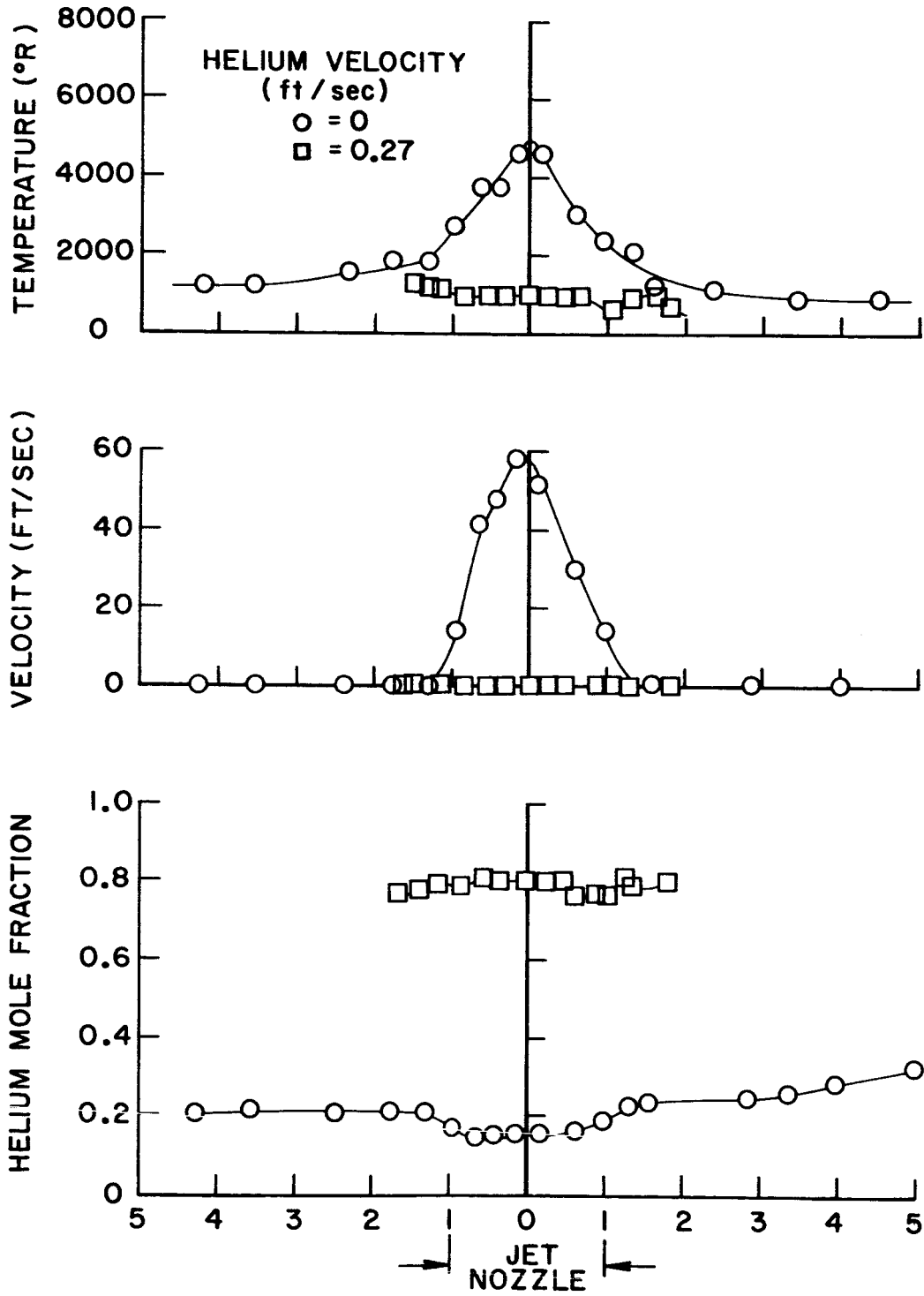
TEMPERATURE, VELOCITY AND COMPOSITION PROFILES AT 1 INCH DOWNSTREAM FROM NOZZLE EXIT PLANE

FIGURE 24



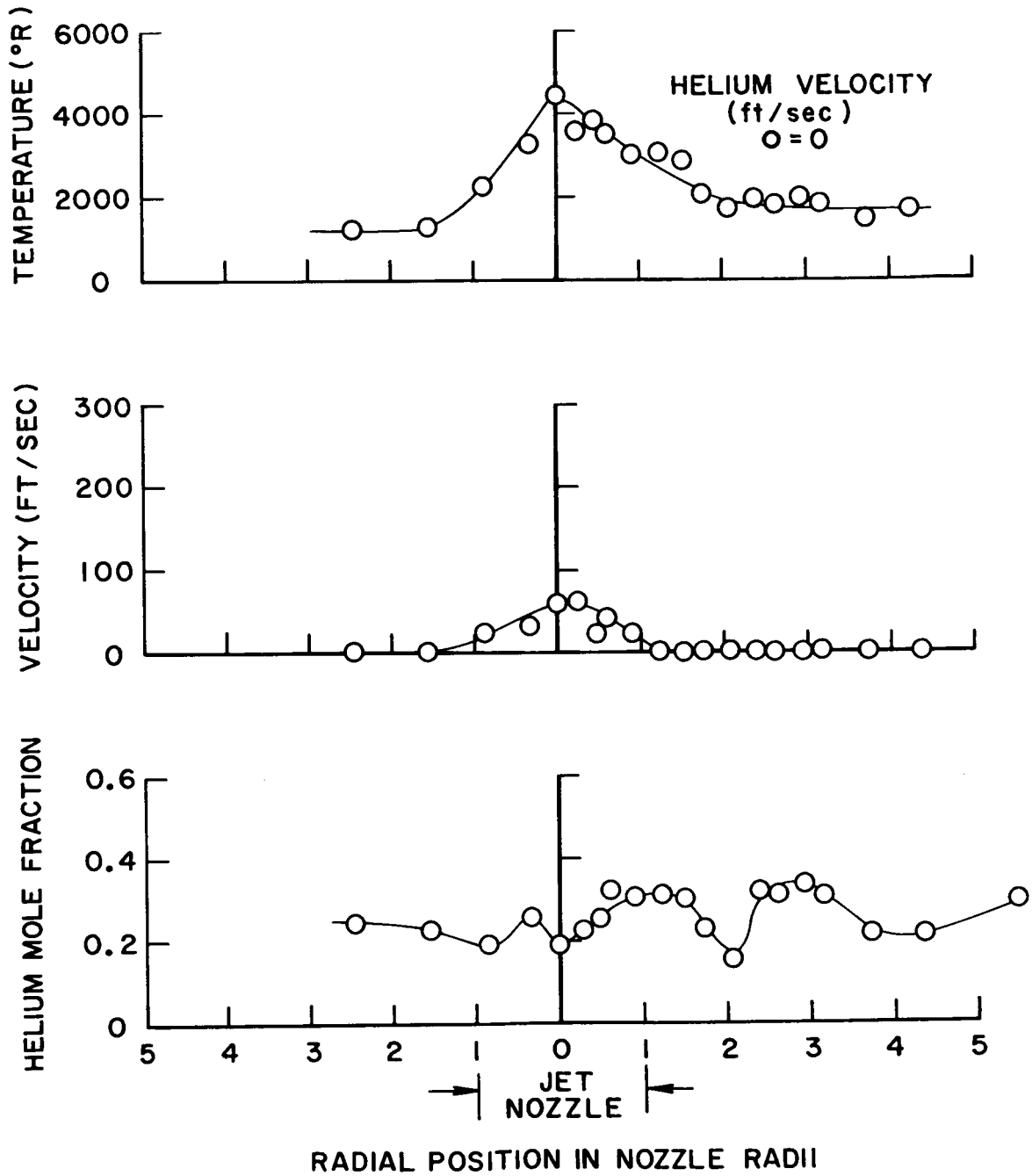
TEMPERATURE, VELOCITY AND COMPOSITION PROFILES
AT 2 INCHES DOWNSTREAM FROM NOZZLE EXIT PLANE

FIGURE 25



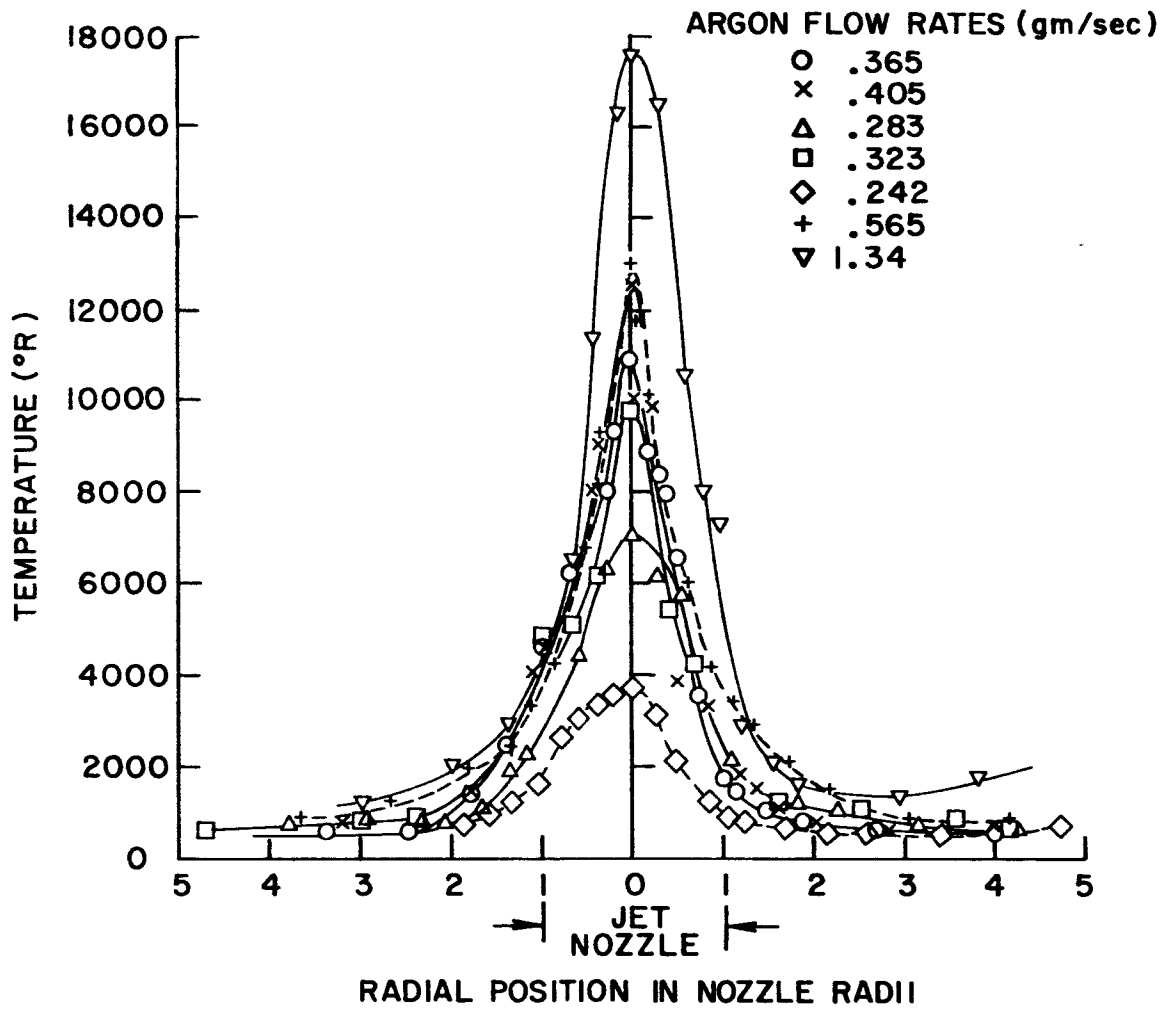
TEMPERATURE, VELOCITY AND COMPOSITION PROFILES AT 3 INCHES DOWNSTREAM FROM NOZZLE EXIT PLANE

FIGURE 26



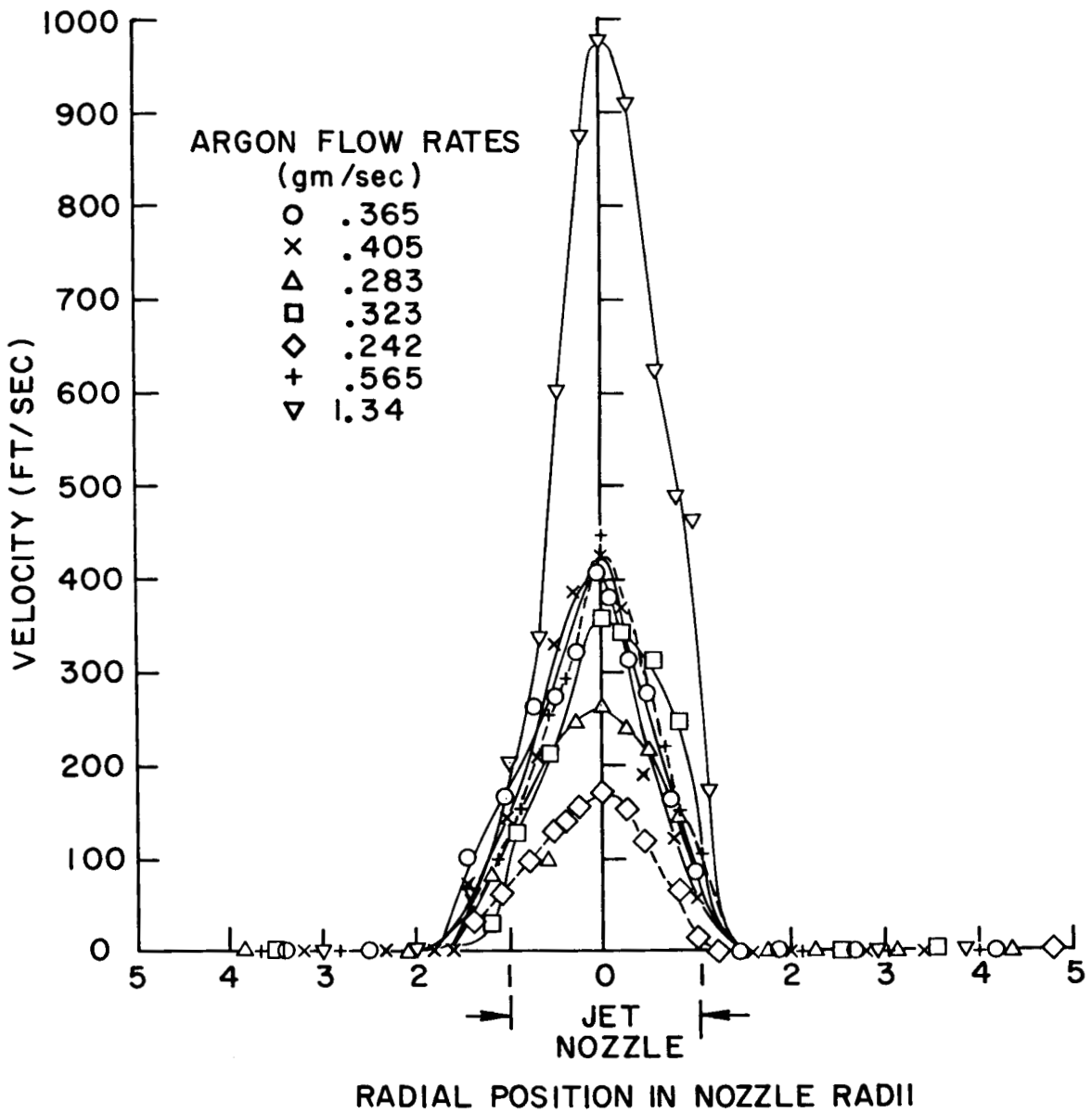
TEMPERATURE, VELOCITY AND COMPOSITION PROFILES AT 5 INCHES DOWNSTREAM FROM NOZZLE EXIT PLANE

FIGURE 27



TEMPERATURE PROFILE AT ONE INCH DOWNSTREAM FROM NOZZLE EXIT PLANE FOR VARIABLE ARGON FLOW (HELIUM VELOCITY = 0.27 FT/SEC)

FIGURE 28



VELOCITY PROFILE AT ONE INCH DOWNSTREAM FROM NOZZLE EXIT PLANE FOR VARIABLE ARGON FLOW (HELIUM VELOCITY = 0.27 FT/SEC)

FIGURE 29

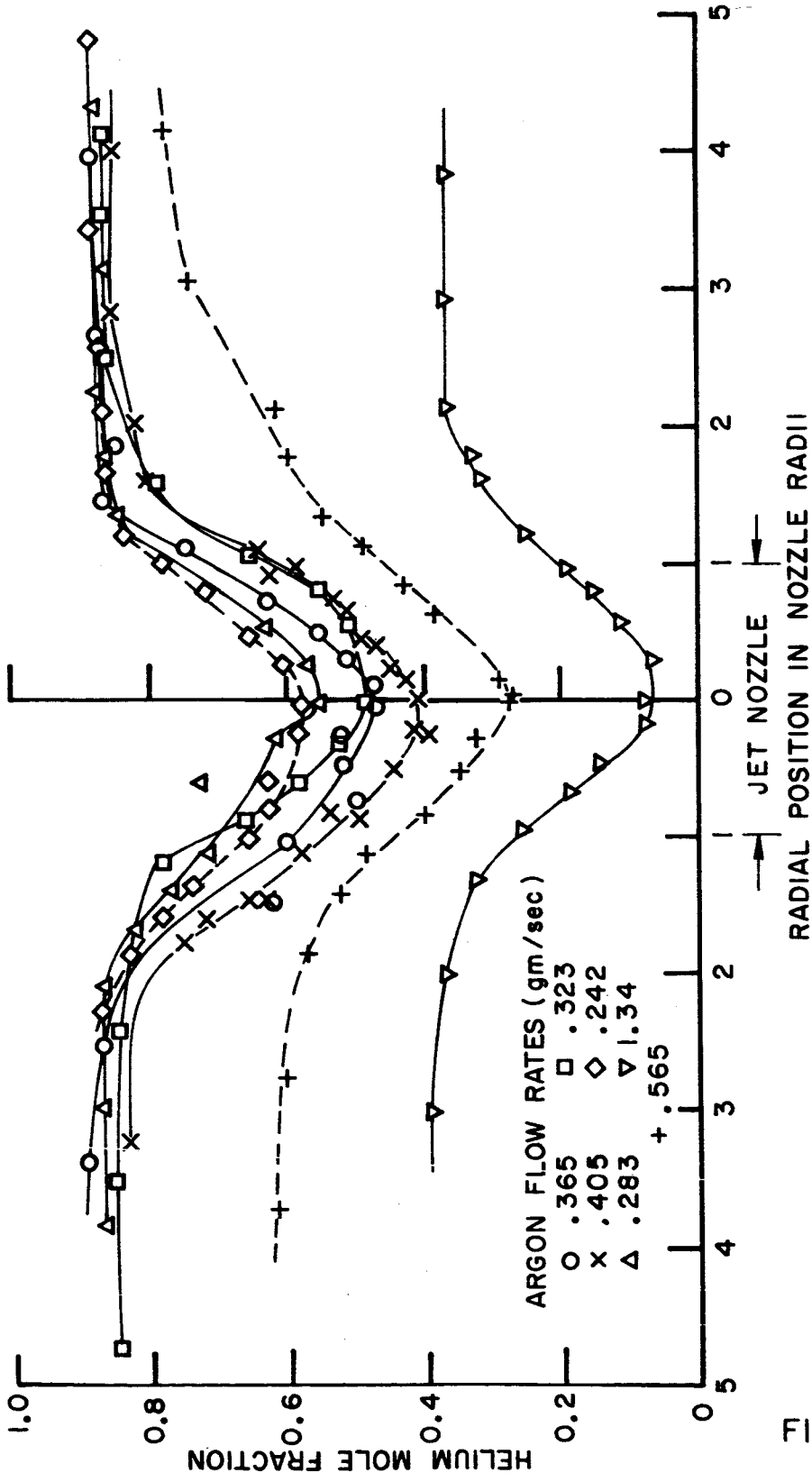


FIGURE 30
COMPOSITION PROFILE AT ONE INCH DOWNSTREAM
FROM NOZZLE EXIT PLANE FOR VARIABLE ARGON FLOW
(HELIUM VELOCITY = 0.27 FT/SEC)

NASA Lewis Research Center
21000 Brookpark Rd.
Cleveland, Ohio 44135
Attn: Norman Musial (MS 5-5)

NASA Scientific and Technical
Information Facility (6)
Box 5700
Bethesda, Md.
Attn: NASA Representative

NASA Lewis Research Center (2)
21000 Brookpark Rd.
Cleveland, Ohio 44135
Attn: Library (3-7)

NASA Lewis Research Center
21000 Brookpark Rd.
Cleveland, Ohio 44135
Attn: Report Control Office (5-5)

Jet Propulsion Laboratory
Propulsion Division
Pasadena, California 91103
Attn: Mr. D. R. Bartz
Manager, Research and Advanced
Concepts Section

Air Force Institute of Technology
Wright-Patterson Air Force Base, Ohio
Attn: Dr. Charles J. Bridgman
Assoc. Professor of Physics

The Boeing Company
Seattle, Washington 98124
Attn: Mr. J. A. Brousseau (MS 47-18)
Propulsion Systems Technology

United Aircraft Corporation
Research Laboratories
400 Main Street
East Hartford, Connecticut 06108
Attn: Dr. Wayne G. Burwell

Electro-Optical Systems, Inc.
300 N. Haistead Street
Pasadena, California 91107
Attn: Dr. Robert W. Bussard

Aerojet-General Corporation
REON Division
Sacramento, California
Attn: Mr. James Carton, Advanced Concepts

Illinois Institute of Technology
Chicago, Illinois 60616
Attn: Dr. Peter Chiarulli, Head
Mechanics Department

Los Alamos Scientific Laboratory
Los Alamos, New Mexico
Attn: Dr. Ralph Cooper
T Division

Aerospace Corporation
Post Office Box 95085
Los Angeles, California 90045
Attn: Mr. Holmes F. Crouch
Systems Research and Planning Division

Jet Propulsion Laboratory
4800 Oak Grove Drive
Pasadena, California
Attn: Mr. Jerry P. Davis
Bldg. 122-3

Rocketdyne
6633 Canoga Avenue
Canoga Park, California
Attn: Dr. Robert Dillaway
Nucleonics Department

Westinghouse Electric Corporation
Pittsburgh, Pennsylvania 15236
Attn: Dr. D. W. Drawbaugh
Astronuclear Laboratory

Illinois Institute of Technology
Chicago, Illinois 60616
Attn: Dr. Andrew Fejer, Head
Mechanical and Aerospace
Engineering Department

United Aircraft Corporation
Research Laboratories
400 Main Street
East Hartford, Connecticut 06108
Attn: Dr. William M. Foley

Institute for Defense Analysis
1666 Connecticut Avenue, NW
Washington, 9, D.C.
Attn: Dr. Robert H. Fox

Oak Ridge National Laboratory
P. O. Box Y
Oak Ridge, Tennessee 37831
Attn: Mr. A. P. Fraas

Catholic University
Washington, D. C.
Attn: Dr. C. C. Chang
Head, Space Sciences & Applied Physics

Space Technology Laboratories
One Space Park
Redondo Beach, California
Attn: Mr. L. A. Gore

D. A. S. A.
Pentagon
Washington, D. C.
Attn: Dr. Theodore B. Taylor

Princeton University
Forrestal Research Center
Princeton, New Jersey
Attn: Professor Jerry Grey

Columbia University
School of Engineering and
Applied Science
New York, N. Y. 10027
Attn: Professor Robert A. Gross

Research Institute of Temple
University
Philadelphia, Pennsylvania
Attn: Dr. A. V. Grosse

Los Alamos Scientific Laboratory
P. O. Box 1663
Los Alamos, New Mexico
Attn: Dr. George Grover (N-5)

Rocketdyne
Canoga Park, California
Attn: Dr. S. V. Gunn

Massachusetts Institute of Technology
Cambridge, Massachusetts 02139
Attn: Professor Elias P. Gyftopoulos
Room 24-109

Lawrence Radiation Laboratory
P. O. Box 808
Livermore, California
Attn: Dr. James Hadley

Brookhaven National Laboratory
Upton, Long Island, New York
Attn: Mr. L. P. Hatch

Jet Propulsion Laboratory
4800 Oak Grove Drive
Pasadena, California
Attn: Dr. Clifford J. Heindl
Bldg. 83-210

Douglas Aircraft Company
Missiles and Space Systems Division
Santa Monica, California
Attn: Dr. R. J. Holl

REON
Aerojet-General Corporation
Sacramento, California
Attn: Mr. William Houghton

Space Technology Laboratory
One Space Park
Redondo Beach, California
Attn: Mr. Henry Hunter

Bellcom, Inc.
Washington, D. C.
Attn: Mr. Maxwell Hunter

Massachusetts Institute of Technology
Cambridge, Massachusetts 02139
Att. Professor Abraham Hyatt
Room 33-113

Advanced Space Technology, A2-263
Douglas Missiles & Space Systems Div.
Santa Monica, California
Attn: Dr. Kurt P. Johnson

Rocketdyne Division of North
American Aviation
6633 Canoga Avenue
Canoga Park, California
Attn: Mr. Carmen Jones

NASA Marshall Space Flight Center
Nuclear Vehicle Projects Office
M-P & VE-NP
Propulsion & Vehicle Engineering Div.
Huntsville, Alabama
Attn: Mr. W. Y. Jordan

Aerospace Research Laboratories (ARN)
Wright-Patterson AFB
Ohio 45433
Attn: Lt. Col. M. R. Keller

Massachusetts Institute of Technology
Cambridge, Massachusetts 02139
Attn: Professor J. L. Kerrebrock
Room 33-115

Oak Ridge National Laboratory
Reactor Division
P. O. Box Y
Oak Ridge, Tennessee 37831
Attn: Dr. John J. Keyes, Jr.

Douglas Aircraft Company
Missiles and Space Systems Division
Santa Monica, California
Attn: Dr. D. E. Knapp

TWR/Space Technology Laboratory
Propulsion Laboratory
Building S
One Space Park
Redondo Beach, California
Attn: Mr. Water F. Krieve

Aerospace Corporation
Fluid Dynamics Section
P. O. Box 95085
Los Angeles, California 90045
Attn: Dr. W. S. Lewellyn, Manager

Massachusetts Institute of Technology
Cambridge, Massachusetts 02139
Attn: Professor Edward Mason (NW12)

United Aircraft Corporation
Research Laboratories
400 Main Street
East Hartford, Connecticut 06108
Attn: Mr. George H. McLafferty

Jet Propulsion Laboratory
4800 Oak Grove Avenue
Pasadena, California
Attn: Dr. Robert V. Meghreblian

Oak Ridge National Laboratory
P. O. Box Y
Oak Ridge, Tennessee 37831
Attn: Dr. A. J. Miller

General Atomic
P. O. Box 608
San Diego 12, California
Attn: Mr. James Nance

Georgia Institute of Technology
Chemical Engineering Department
Atlanta 13, Georgia
Attn: Professor Clyde Orr, Jr.

United Aircraft Corporation
Research Laboratories
400 Main Street
East Hartford, Connecticut 06108
Attn: Mr. Frank S. Owen

Oak Ridge National Laboratory
P. O. Box X
Oak Ridge, Tennessee 37831
Attn: Mr. P. Patriarca

RAND Corporation
Santa Monica, California
Attn: Dr. Ben Pinkel

NASA Lewis Research Center
Nuclear Reactor Division
21000 Brookpark Road
Cleveland, Ohio 44135
Attn: Mr. Robert G. Ragsdale (MS 49-2)

NASA Lewis Research Center
Nuclear Reactor Division
21000 Brookpark Road
Cleveland, Ohio 44135
Attn: Mr. Frank E. Rom (MS 49-2)

The Boeing Company
Advanced Nuclear Group
Seattle, Washington 98124
Attn: Dr. J. B. Romero

Avco Everett Research Laboratory
Everett, Massachusetts
Attn: Dr. Richard Rosa

General Motors
Allison Division
Indianapolis, Indiana
Attn: Mr. Eli Roth

Aerospace Corporation
Aerodynamic & Heat Transfer Dept.
P. O. Box 95085
Los Angeles, California 90045
Attn: Dr. Martin Rosenzweig

Aerojet-General Corporation
REON Division
Reactor Coordination Department
Sacramento, California
Attn: Mr. C. K. Sappett

Oak Ridge National Laboratory
P. O. Box Y
Oak Ridge, Tennessee 37831
Attn: Mr. H. W. Savage

AEC/NASA Space Nuclear Propulsion
Office
Division of Reactor Development
U. S. Atomic Energy Commission
Washington, D. C.
Attn: Mr. F. C. Schwenk

Jet Propulsion Laboratory
Space Sciences Division
Pasadena 3, California
Attn: Dr. Henry Stumpf

Space Technology Laboratories
One Space Park
Redondo Beach, California
Attn: Mr. T. Szekely

National Aeronautics and Space Council
Executive Office Building
White House Post Office
Washington, D. C.
Attn: Dr. Robert F. Trapp

University of Florida
Dept. of Nuclear Engineering
Gainesville, Florida
Attn: Dr. Robert Uhrig, Chairman

Aerospace Research Laboratories (ARD-1)
Wright-Patterson AFB
Ohio 45433
Attn: Dr. Hans von Ohain

Illinois Institute of Technology
Chemical Engineering Department
Chicago, Illinois 60616
Attn: Dr. H. Weinstein

Princeton University
Department of Physics
Princeton, N. J.
Attn: Professor E. P. Wigner

AEC/NASA Space Nuclear Propulsion
Office
Division of Reactor Development
U. S. Atomic Energy Commission
Washington, D. C.
Attn: Captain William Yingling

Purdue University
Mechanical Engineering Department
Lafayette, Indiana 47907
Attn: Professor M. J. Zucrow
Atkins Professor of Engineering